To Harvest and Jam: A Paradigm of Self-Sustaining Friendly Jammers for Secure AF Relaying

Hong Xing, *Student Member, IEEE*, Kai-Kit Wong, *Senior Member, IEEE*, Zheng Chu, and Arumugam Nallanathan, *Senior Member, IEEE*

***Abstract*—This paper studies the use of multi-antenna *harvest-and-jam (HJ)* helpers in a multi-antenna amplify-and-forward (AF) relay wiretap channel assuming that the direct link between the source and destination is broken. Our objective is to maximize the secrecy rate at the destination subject to the transmit power constraints of the AF relay and the HJ helpers. In the case of perfect channel state information (CSI), the joint optimization of the artificial noise (AN) covariance matrix for cooperative jamming and the AF beamforming matrix is studied using semidefinite relaxation (SDR) which is tight, while suboptimal solutions are also devised with lower complexity. For the imperfect CSI case, we provide the equivalent reformulation of the worst-case robust optimization to maximize the minimum achievable secrecy rate. Inspired by the optimal solution to the case of perfect CSI, a suboptimal robust scheme is proposed striking a good tradeoff between complexity and performance. Finally, numerical results for various settings are provided to evaluate the proposed schemes.**

***Index Terms*—Amplify-and-forward relay, artificial noise, cooperative jamming, harvest-and-jam, physical-layer security, robust optimization, semidefinite relaxation, wireless energy transfer.**

I. Introduction

THE pressing demand for high data rate in wireless communications networks coupled with the fact that mobile devices are physically small and power-limited by batteries, has driven the notion of energy harvesting (EH) to become a promising resolution for green communications [1], [2]. Among the varied available resources for EH, radio-frequency (RF)-enabled wireless energy transfer (WET) has aroused an upsurge of interest for its long operation range, ubiquitous existence in the electromagnetic radiation, and effective energy multicasting, which motivates the paradigm of simultaneous wireless information and power transfer (SWIPT), e.g., [3]–[6].

A typical SWIPT system consists of one access point (AP) that has constant power supply and broadcasts wireless signals to a group of user terminals, amongst which some intend to decode information, referred to as information receivers (IRs), while others scavenge energy from the ambient radio signals, named energy receivers (ERs). This gives rise to a challenging physical (PHY)-layer security issue where the ERs may eavesdrop the information sent to the IRs due to their close proximity to the AP To overcome this problem, in [7]–[9], several researchers presented various approaches to guarantee secret communication to the IRs and maximize the energy simultaneously transferred to the ERs or to satisfy the individual EH requirement for the ERs and maximize the secrecy rate for the IR, by advocating the dual use of the artificial noise (AN) or jamming.

However, previous works all assumed that the ERs in the SWIPT systems attempt to intercept the information for the IR, which is overly protective. On the contrary, it is possible that some ERs are cooperative, especially when they are EH-enabled wirelessly. Following the recent advances in *wireless powered communications networks* [10], [11], this paper proposes a self-sustaining *harvest-and-jam (HJ)* relaying protocol, where in the first transmission phase a single-antenna transmitter transfers confidential information to a multiple-antenna amplify-and-forward (AF) relay and power to a group of multi-antenna EH-enabled idle helpers simultaneously, while in the second phase, the relay amplifies and forwards the information to the IR under the protection of the AN generated by the helpers using the energy harvested from their received signals in the first transmission phase.

Physical (PHY)-layer security issues in the rapidly growing cooperative networks have attracted much attention. Cooperative approaches, such as, *cooperative jamming*, communications have been widely examined [12]–[15]. The idea is to assist the transmitter in the secrecy transmission by generating an AN to interfere with the eavesdropper via either multiple antennas or external trusted helpers [16]–[19]. However, all of those utilizing ANs require additional supply of power and therefore incur extra system costs. Meanwhile, collaborative use of relays to form effective beams jamming the eavesdropper, i.e., *secure collaborative relay beamforming*, has been studied for relay-wiretap channels with single eavesdropper in [20], multiple eavesdroppers with AF relays and decode-and-forward (DF) relays in [21] and [22], respectively. All, however,

Manuscript received February 26, 2015; revised July 06, 2015 and August 26, 2015; accepted August 28, 2015. Date of publication September 10, 2015; date of current version November 12, 2015. The associate editor coordinating the review of this manuscript was Prof. Rui Zhang. This work was supported in part by the China Scholarship Council (CSC), in part by the U.K. Engineering and Physical Sciences Research Council (EPSRC) under Grant EP/K015893/1, and in part by the EPSRC under Grant EP/M016145/1. This paper has been presented in part at the IEEE Global Communications Conference (GLOBECOM), Austin, TX, USA, December 8–12, 2014. (*Corresponding authors: K.-K. Wong and Z. Chu.*)

H. Xing and A. Nallanathan are with the Centre for Telecommunications Research, King's College London, London WC2R 2LS, U.K. (e-mail: hong.xing@kcl.ac.uk; arumugam.nallanathan@kcl.ac.uk).

K.-K. Wong is with the Department of Electronic and Electrical Engineering, University College London, London WC1E 6BT, U.K. (e-mail: kai-kit.wong@ucl.ac.uk).

Z. Chu is with the School of Electrical and Electronic Engineering, Newcastle University, Newcastle NE1 7RU, U.K. (e-mail: z.chu@ncl.ac.uk).

Color versions of one or more of the figures in this paper are available online at http://ieeexplore.ieee.org.

Digital Object Identifier 10.1109/TSP.2015.2477800

This work is licensed under a Creative Commons Attribution 3.0 License. For more information, see http://creativecommons.org/licenses/by/3.0/

assumed the availability of perfect channel state information (CSI). Though [23] proposed robust AF relay beamforming against the eavesdropper's channel, the solutions were yet suboptimal.

The assumption of perfect CSI of the eavesdroppers appears to be too ideal because the eavesdroppers, despite being legitimate users, wish to hide from the transmitter without being cooperative in the stage of channel estimation. Even if they are registered users and bound to help the transmitter in obtaining their CSIs to facilitate their own communication, the CSIs at the transmitter side will change due to mobility and Doppler effect, and may be outdated. Moreover, even for the legitimate users, the estimated CSIs may also be subject to quantization errors due to the limited capacity of the feedback channel, although the inaccuracy is reasonably assumed less severe than that for the eavesdroppers. To tackle this issue, state-of-art schemes have been developed ([24] and the references therein), among which the *worst-case secrecy rate* is commonly employed to formulate the robust secrecy rate maximization problem [8], [19], [25]–[27]. The robust transmit covariance design for the secrecy rate maximization in a multiple-input-single-output (MISO) channel overheard by multi-antenna eavesdroppers was considered in [25], [28] while the enhanced secrecy performance was achieved by introducing a friendly jammer in the same scenario in [26], in which a joint optimization of the robust transmit covariance and power allocation between the source and the helper was studied via geometric programming. More recently, [8] studied a joint robust design of the information beams, the AN and the energy signals for SWIPT networks with quality-of-service (QoS) constraints.

The contribution of this paper is threefold. First, with perfect CSI, in addition to the joint optimal solutions, we propose two near-optimal schemes with much reduced complexity by exploiting the optimal structure of the relay weight matrix, and providing a semi-closed form solution for the relay weight matrix given fixed *null-space* jamming, respectively. Second, besides the imperfect eavesdropper's channel, legitimate channels such as those from the K HJ helpers (the transmitter) to the legitimate receiver (K HJ helpers), and from the AF relay to the receiver are jointly modeled with imperfect estimation, and multiple semi-indefinite non-convex constraints have been judiciously replaced by linear matrix inequalities (LMIs) to fit the semi-definite programming (SDP). Third, a rank-one reconstruction algorithm exploiting the structure of the semi-definite relaxation (SDR)-based solutions has been proposed to provide promising performance at low computational cost.

Of particular relevance to our work is [29] which jointly optimizes the AF matrices and AN covariances in a relay wiretap channel with multiple multi-antenna AF relays and multiple multi-antenna eavesdroppers via a worst-case robust formulation. While our network model is similar, the difference of our work from [29] is twofold. On one hand, in this paper, the AN generated by the friendly jammers are subject to their respective channels from the transmitter during WET in the first transmission phase. On the other hand, the technique in [29, Proposition 1] cannot be applied to our problem since the AN beams and the forwarded information are transmitted via different channels in ours. As a consequence, to the best of authors' knowledge, our proposed worst-case based *robust* optimization scheme that incorporates imperfect CSIs into all the HJ helpers, has not been addressed in the literature.

It is worth noting that devising a wireless-powered friendly jammer to enhance PHY-layer security for a direct transmission protocol was studied in [30], in which the "harvesting" blocks and "jamming" blocks were well exploited to compose four different types of harvesting-jamming cycles. Compared to [30], which focused on the dedicated scheduling of "harvest" and "jam" operations and its long-term performance, ours are concerned with adaptive rate/power optimization with multiple HJ helpers to achieve higher worst-case secrecy rate. Moreover, instead of assuming perfect channels to/from the HJ helpers, our *robust* optimization algorithm takes imperfect legitimate channels into account to provide robustness.

Note that in this paper, as in [23], [29], we assume that the channel between the transmitter and the AF relay is perfectly known and there is no direct link between the transmitter and the receiver or the eavesdropper, a common assumption in the concerned AF relay wiretap channel [20], [21].

Notations: Throughout, we use the upper case boldface letters for matrices and lower case boldface letters for vectors. The superscripts $(\cdot)^T$, $(\cdot)^\dagger$ and $(\cdot)^H$ represent the transpose, conjugate and conjugate transpose, respectively. Also, $\mathrm{tr}(\cdot)$ and $\mathbb{E}[\cdot]$ stand for the trace of a matrix and the statistical expectation for random variables, respectively. Likewise, $\mathrm{vec}(\boldsymbol{A})$ is defined as a column vector obtained by stacking the rows of $\boldsymbol{A}$ on top of one another. $\mathrm{vec}^{(-1)}$ is the inverse operation of vec. $\mathbf{null}(\boldsymbol{A})$ denotes the null space of $\boldsymbol{A}$. $\otimes$ represents the Kronecker product of two matrices. In addition, the notation $\boldsymbol{A} \succeq 0$ indicates that $\boldsymbol{A}$ is a positive semi-definite matrix and $\boldsymbol{I}(\mathbf{0})$ denotes an identity (all-zero) matrix with appropriate size. Furthermore, $\|\cdot\|$ represents the Euclidean norm of a vector, while $P_r(\cdot)$ stands for the probability of an input random event. Finally, $[x]^+$ denotes $\max(0, x)$ and $(\cdot)^*$ stands for an optimal solution.

II. Network Model

We consider a cooperative relay wiretap channel for SWIPT over a given frequency band as shown in Fig. 1(a). We assume that there is a transmitter, named Alice, sending confidential messages to the IR, Bob, in the presence of an eavesdropper [31], Eve, with the aid of a multi-antenna AF relay and K ERs willing to act as HJ helpers, $\mathcal{H}_{\mathrm{helper}} = \{\mathsf{H}_1, \ldots, \mathsf{H}_K\}$. The transmitter, ERs, and the AF relay are deployed in a same cluster that is relatively far away from the destination and Eve, such that there is no direct link from the transmitter to the receiver or Eve, respectively. Moreover, the ERs are assumed to be located closer to the transmitter than the AF relay in order that they can harvest sufficient amount of energy for jamming. Alice, Bob and Eve are all assumed to be equipped with single antenna, while the AF relay and each of the K helpers are assumed to have the same N_t antennas.

Using two equal slots for the HJ relaying protocol, as shown in Fig. 1(b), for the first phase, Alice sends a confidential message to the relay while simultaneously transferring energy to the K helpers; for the second phase, the relay amplifies and forwards the message to Bob while the K helpers perform cooperative jamming using their respective harvested energy from the first transmission phase, to compromise Eve. In this paper, we

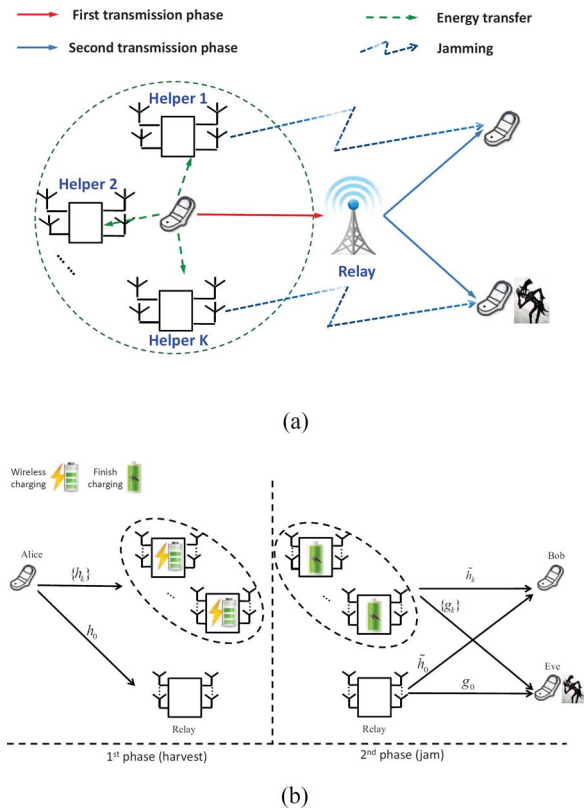

Fig. 1. HJ-enabled cooperative relaying for secure SWIPT.(a) AF-relaying wiretap channel with jamming. (b) The HJ relaying protocol.

assume a quasi-static fading environment and for convenience denote $\boldsymbol{h}_0 \in \mathbb{C}^{N_t \times 1}$ as the complex channel from the transmitter to the relay and $\boldsymbol{h}_k \in \mathbb{C}^{N_t \times 1}$, $k = 1, \ldots, K$, as that from the transmitter to the kth helper; $\tilde{\boldsymbol{h}}_0$ as the transpose of the complex channel from the relay to Bob and $\tilde{\boldsymbol{h}}_k \in \mathbb{C}^{N_t \times 1}$, $k = 1, \ldots, K$, as that from H_k to Bob; $\boldsymbol{g}_0 \in \mathbb{C}^{N_t \times 1}$ and $\boldsymbol{g}_k \in \mathbb{C}^{N_t \times 1}$, $k = 1, \ldots, K$, as those from the relay and H_k to Eve, respectively.

In the first transmission phase, the baseband received signal at the AF relay can be expressed as

$$\boldsymbol{y}_r = \boldsymbol{h}_0 \sqrt{P_s} s + \boldsymbol{n}_r, \tag{1}$$

where s is a circularly symmetric complex Gaussian (CSCG) random variable, denoted by $s \sim \mathcal{CN}(0, 1)$ and $\boldsymbol{n}_r$ is the additive complex noise vector, denoted by $\boldsymbol{n}_r \sim \mathcal{CN}(\boldsymbol{0}, \sigma_r^2 \boldsymbol{I})$. Also, P_s denotes the given transmit power at Alice. Further, the received signal at each helper H_k is expressed as

$$\boldsymbol{y}_k = \boldsymbol{h}_k \sqrt{P_s} s + \boldsymbol{n}'_k, \tag{2}$$

where $\boldsymbol{n}'_k$ is the additive noise, denoted by $\boldsymbol{n}'_k \sim \mathcal{CN}(\boldsymbol{0}, \sigma_h^2 \boldsymbol{I})$.

On the other hand, for WET, the harvested energy of H_k in each unit slot is given by

$$E_k = \eta \mathbb{E}[\|\boldsymbol{h}_k \sqrt{P_s} s\|^2] = \eta P_s \|\boldsymbol{h}_k\|^2, \forall k, \tag{3}$$

where $0 < \eta \leq 1$ denotes the EH efficiency.

In the second transmission phase, the linear operation at the AF relay can be represented by

$$\boldsymbol{x}' = \boldsymbol{W} \boldsymbol{y}_r, \tag{4}$$

where $\boldsymbol{x}' \in \mathbb{C}^{N_t \times 1}$ is the retransmit signal at the AF relay and $\boldsymbol{W} \in \mathbb{C}^{N_t \times N_t}$ is the beamforming matrix. Note that the transmit power of the AF relay can be shown as

$$\operatorname{tr}\left(\mathbb{E}\left[\boldsymbol{x}\boldsymbol{x}^H\right]\right) = \operatorname{tr}\left(\boldsymbol{W}\left(P_s \boldsymbol{h}_0 \boldsymbol{h}_0^H + \sigma_r^2 \boldsymbol{I}\right) \boldsymbol{W}^H\right), \tag{5}$$

which is constrained by the maximum available power at the AF relay, i.e., P_r, which is given by

$$\operatorname{tr}\left(\boldsymbol{W}\left(P_s \boldsymbol{h}_0 \boldsymbol{h}_0^H + \sigma_r^2 \boldsymbol{I}\right) \boldsymbol{W}^H\right) \leq P_r. \tag{6}$$

In the meantime, each H_k will help generate an AN $\boldsymbol{n}_k \in \mathbb{C}^{N_t \times 1}$ to interfere with Eve. Similar to [16], we assume that $\boldsymbol{n}_k$'s are independent CSCG vectors denoted by $\boldsymbol{n}_k \sim \mathcal{CN}(0, \boldsymbol{Q}_k)$, $\forall k$, since the worst-case noise for Eve is known to be Gaussian. In addition, each H_k has a transmit power constraint due to its harvested energy in the previous transmission phase, i.e., $\operatorname{tr}(\boldsymbol{Q}_k) \leq \eta P_s \|\boldsymbol{h}_k\|^2$ (cf. Equation (3)), $\forall k$.

The received signal at Bob can thus be expressed as

$$\boldsymbol{y}_b = \sqrt{P_s} \tilde{\boldsymbol{h}}_0^T \boldsymbol{W} \boldsymbol{h}_0 s + \sum_{k=1}^{K} \tilde{\boldsymbol{h}}_k^T \boldsymbol{n}_k + \tilde{\boldsymbol{h}}_0^T \boldsymbol{W} n_r + \boldsymbol{n}_b, \tag{7}$$

where $\boldsymbol{n}_b \sim \mathcal{CN}(0, \sigma_b^2 \boldsymbol{I})$ is the additive noise at Bob. Similarly, the received signal at Eve can be expressed as

$$\mathbf{y}_e = \sqrt{P_s} \boldsymbol{g}_0^T \boldsymbol{W} \boldsymbol{h}_0 s + \sum_{k=1}^{K} \boldsymbol{g}_k^T \boldsymbol{n}_k + \boldsymbol{g}_0^T \boldsymbol{W} \boldsymbol{n}_r + \boldsymbol{n}_e, \tag{8}$$

where $\boldsymbol{n}_e \sim \mathcal{CN}(0, \sigma_e^2 \boldsymbol{I})$. According to (7) and (8), the signal-to-interference-plus-nose-ratio (SINR) at Bob and Eve can be, respectively, expressed as

$$\gamma_b = \frac{P_s |\tilde{\boldsymbol{h}}_0^T \boldsymbol{W} \boldsymbol{h}_0|^2}{\sigma_r^2 \tilde{\boldsymbol{h}}_0^T \boldsymbol{W} \boldsymbol{W}^H \tilde{\boldsymbol{h}}_0^\dagger + \sum_{k=1}^{K} \tilde{\boldsymbol{h}}_k^T \boldsymbol{Q}_k \tilde{\boldsymbol{h}}_k^\dagger + \sigma_b^2}, \tag{9}$$

and

$$\gamma_e = \frac{P_s |\boldsymbol{g}_0^T \boldsymbol{W} \boldsymbol{h}_0|^2}{\sigma_r^2 \boldsymbol{g}_0^T \boldsymbol{W} \boldsymbol{W}^H \boldsymbol{g}_0^\dagger + \sum_{k=1}^{K} \boldsymbol{g}_k^T \boldsymbol{Q}_k \boldsymbol{g}_k^\dagger + \sigma_e^2}. \tag{10}$$

As such, the achievable secrecy rate at Bob is [16]

$$r_0 = \frac{1}{2}[\log_2(1 + \gamma_b) - \log_2(1 + \gamma_e)]^+. \tag{11}$$

III. Joint AN-AF Beamforming With Perfect CSI

A. Problem Formulation for Perfect CSI

We aim to maximize the secrecy rate at Bob subject to the transmit power constraints at the AF relay and each individual helper H_k, $k = 1, \ldots, K$. Thus, our problem is to solve

$$\begin{aligned} (\mathrm{P1}): \max_{\{\boldsymbol{Q}_k\}, \boldsymbol{W}} \quad & r_0 \\ \text{s.t.} \quad & (6), && \text{(12a)} \\ & \operatorname{tr}(\boldsymbol{Q}_k) \leq \eta P_s \|\boldsymbol{h}_k\|^2, \forall k, && \text{(12b)} \\ & \boldsymbol{Q}_k \succeq \boldsymbol{0}, \forall k. && \text{(12c)} \end{aligned}$$

Next, we define a new function $\bar{F}(\{\boldsymbol{Q}_k\}, \boldsymbol{W})$ as

$$\bar{F}(\{\boldsymbol{Q}_k\}, \boldsymbol{W}) \triangleq \frac{1 + \gamma_b}{1 + \gamma_e}. \tag{13}$$

It can be easily shown that the optimal solution $\{\boldsymbol{Q}_k^*\}$, $\boldsymbol{W}^*$ to (P1), is also optimal for (P1′) given by

$$(\mathrm{P1}') : \max_{\{\boldsymbol{Q}_k\},\boldsymbol{W}} \bar{F}(\{\boldsymbol{Q}_k\},\boldsymbol{W}) \ \mathtt{s.t.}(12a)\text{–}(12c). \tag{14}$$

Hence, we focus on solving problem (P1′) in the rest of the paper. However, since (P1′) is in general a non-convex problem that is hard to solve, we will reformulate it into a two-stage optimization problem. First, we constrain the SINR at Eve to be $\bar{\gamma}_e$, it thus follows from (13) that $\bar{F}(\{\overline{\boldsymbol{Q}}_k\},\boldsymbol{W})$ is maximized when γ_b is maximized, which can be obtained by solving the following problem:

$$\begin{aligned}(\mathrm{P1}'.1) : &\max_{\{\boldsymbol{Q}_k,\boldsymbol{W}\}} \frac{P_s|\tilde{\boldsymbol{h}}_0^T\boldsymbol{W}\boldsymbol{h}_0|^2}{\sigma_r^2\tilde{\boldsymbol{h}}_0^T\boldsymbol{W}\boldsymbol{W}^H\tilde{\boldsymbol{h}}_0^\dagger+\sum_{k=1}^K\tilde{\boldsymbol{h}}_k^T\boldsymbol{Q}_k\tilde{\boldsymbol{h}}_k^\dagger+\sigma_b^2}\\ \mathtt{s.t.}&\frac{P_s|\boldsymbol{g}_0^T\boldsymbol{W}\boldsymbol{h}_0|^2}{\sigma_r^2\boldsymbol{g}_0^T\boldsymbol{W}\boldsymbol{W}^H\boldsymbol{g}_0^\dagger+\sum_{k=1}^K\boldsymbol{g}_k^T\boldsymbol{Q}_k\boldsymbol{g}_k^\dagger+\sigma_e^2}=\bar{\gamma}_e,\\ &(12a)\text{–}(12c).\end{aligned} \tag{15}$$

Let $H(\bar{\gamma}_e)$ denote the optimal value of (P1′.1) given $\bar{\gamma}_e$. Then (P1′) can be equivalently solved by

$$(\mathrm{P1}'.2) : \max_{\bar{\gamma}_e>0} \frac{1+H(\bar{\gamma}_e)}{1+\bar{\gamma}_e}. \tag{16}$$

Lemma 3.1: Problem (P1′) has the same optimal value as (P1′.2), and the same optimal solution as (P1′.1) when $\bar{\gamma}_e$ takes the optimal solution for (P1′.2).

Proof: The proof follows from [7, Lemmas 4.1–4.2]. ■

Therefore, (P1′) can be solved in the following two steps. First, given any $\bar{\gamma}_e > 0$, we solve (P1′.1) to attain $H(\bar{\gamma}_e)$; then we solve (P1′.2) to obtain the optimal $\bar{\gamma}_e^*$.

B. Optimal Solution to (P1′.1)

Here, we consider solving problem (P1′.1) by jointly optimizing the covariance matrix for the AN at each of the HJ helper, $\boldsymbol{Q}_k$'s, and the beamforming matrix, $\boldsymbol{W}$. To facilitate the analysis in the sequel, we rewrite the following equations in line with our definition of $\mathrm{vec}(\cdot)$ [32, Chapter 13]:

$$|\tilde{\boldsymbol{h}}_0^T\boldsymbol{W}\boldsymbol{h}_0|^2 = |\mathrm{vec}^T(\tilde{\boldsymbol{h}}_0\boldsymbol{h}_0^T)\mathrm{vec}(\boldsymbol{W})|^2, \tag{17}$$

$$\tilde{\boldsymbol{h}}_0^T\boldsymbol{W}\boldsymbol{W}^H\tilde{\boldsymbol{h}}_0^\dagger = \|\tilde{\boldsymbol{h}}_0^T\otimes\boldsymbol{I}\mathrm{vec}(\boldsymbol{W})\|^2, \tag{18}$$

$$|\boldsymbol{g}_0^T\boldsymbol{W}\boldsymbol{h}_0|^2 = |\mathrm{vec}^T(\boldsymbol{g}_0\boldsymbol{h}_0^T)\mathrm{vec}(\boldsymbol{W})|^2, \tag{19}$$

$$\boldsymbol{g}_0^T\boldsymbol{W}\boldsymbol{W}^H\boldsymbol{g}_0^\dagger = \|\boldsymbol{g}_0^T\otimes\boldsymbol{I}\mathrm{vec}(\boldsymbol{W})\|^2. \tag{20}$$

In addition, $\mathrm{tr}(\boldsymbol{W}(P_s\boldsymbol{h}_0\boldsymbol{h}_0^H+\sigma_r^2\boldsymbol{I})\boldsymbol{W}^H) = \|\boldsymbol{\Phi}\boldsymbol{w}\|^2$, where $\boldsymbol{\Phi} = (\boldsymbol{I}\otimes\boldsymbol{\Theta}^T)^{1/2}$ with $\boldsymbol{\Theta} = P_s\boldsymbol{h}_0\boldsymbol{h}_0^H+\sigma_r^2\boldsymbol{I}$. Hence, (P1′.1) can be rewritten as

$$\begin{aligned}&(\mathrm{P1}'.1\text{-RW}) :\\ &\max_{\boldsymbol{W},\{\boldsymbol{Q}_k\}} \frac{P_s|\boldsymbol{f}_1^T\boldsymbol{w}|^2}{\sigma_r^2\|\boldsymbol{Y}_1\boldsymbol{w}\|^2+\sum_{k=1}^K\tilde{\boldsymbol{h}}_k^T\boldsymbol{Q}_k\tilde{\boldsymbol{h}}_k^\dagger+\sigma_b^2}\\ &\mathtt{s.t.}\frac{P_s|\boldsymbol{f}_2^T\boldsymbol{w}|^2}{\sigma_r^2\|\boldsymbol{Y}_2\boldsymbol{w}\|^2+\sum_{k=1}^K\boldsymbol{g}_k^T\boldsymbol{Q}_k\boldsymbol{g}_k^\dagger+\sigma_e^2}=\bar{\gamma}_e, \quad (21a)\\ &\|\Phi\boldsymbol{w}\|^2 \le P_r,\\ &(12b),(12c) \quad (21b)\end{aligned}$$

in which $\boldsymbol{w} = \mathrm{vec}(\boldsymbol{W})$, $\boldsymbol{f}_1 = \mathrm{vec}(\tilde{\boldsymbol{h}}_0\boldsymbol{h}_0^T)$, $\boldsymbol{f}_2 = \mathrm{vec}(\boldsymbol{g}_0\boldsymbol{h}_0^T)$, $\boldsymbol{Y}_1 = \tilde{\boldsymbol{h}}_0^T\otimes\boldsymbol{I}$ and $\boldsymbol{Y}_2 = \boldsymbol{g}_0^T\otimes\boldsymbol{I}$.

As problem (P1′.1-RW) is non-convex, we define $\boldsymbol{X} \triangleq \boldsymbol{w}\boldsymbol{w}^H$, $\boldsymbol{F}_1 \triangleq \boldsymbol{f}_1^\dagger\boldsymbol{f}_1^T$, $\boldsymbol{F}_2 \triangleq \boldsymbol{f}_2^\dagger\boldsymbol{f}_2^T$, $\overline{\boldsymbol{Y}}_1 \triangleq \boldsymbol{Y}_1^H\boldsymbol{Y}_1$, $\overline{\boldsymbol{Y}}_2 \triangleq \boldsymbol{Y}_2^H\boldsymbol{Y}_2$ and $\overline{\boldsymbol{\Phi}} \triangleq \boldsymbol{\Phi}^H\boldsymbol{\Phi}$. Then by ignoring the rank-one constraint on $\boldsymbol{X}$, (P1′.1-RW) is modified as

$$\begin{aligned}&(\mathrm{P1}'.1\text{-RW-SDR-Eqv}) :\\ &\max_{\boldsymbol{X},\{\boldsymbol{Q}_k\}} \frac{P_s\mathrm{tr}(\boldsymbol{F}_1\boldsymbol{X})}{\sigma_r^2\mathrm{tr}(\overline{\boldsymbol{Y}}_1\boldsymbol{X})+\sum_{k=1}^K\tilde{\boldsymbol{h}}_k^T\boldsymbol{Q}_k\tilde{\boldsymbol{h}}_k^\dagger+\sigma_b^2}\\ &\mathtt{s.t.}P_s\mathrm{tr}(\boldsymbol{F}_2\boldsymbol{X})\\ &\quad=\bar{\gamma}_e\left(\sigma_r^2\mathrm{tr}(\overline{\boldsymbol{Y}}_2\boldsymbol{X})+\sum_{k=1}^K\boldsymbol{g}_k^T\boldsymbol{Q}_k\boldsymbol{g}_k^\dagger+\sigma_e^2\right), \quad (22a)\\ &\quad\mathrm{tr}(\overline{\boldsymbol{\Phi}}\boldsymbol{X}) \le P_r, \quad (22b)\\ &\quad\mathrm{tr}(\boldsymbol{Q}_k) \le \eta P_s\|\boldsymbol{h}_k\|^2, \forall k, \quad (22c)\\ &\quad\boldsymbol{X}\succeq\boldsymbol{0}, \boldsymbol{Q}_k\succeq\boldsymbol{0}, \forall k. \quad (22d)\end{aligned}$$

Problem (P1′.1-RW-SDR-Eqv), via Charnes-Cooper transformation [33], can be equivalently recast as

$$\begin{aligned}&(\mathrm{P1}'.1\text{-RW-SDR}) : \max_{\boldsymbol{X},\{\boldsymbol{Q}_k\},\tau} \quad P_s\mathrm{tr}(\boldsymbol{F}_1\boldsymbol{X})\\ &\mathtt{s.t.}\quad \sigma_r^2\mathrm{tr}(\overline{\boldsymbol{Y}}_1\boldsymbol{X})+\sum_{k=1}^K\tilde{\boldsymbol{h}}_k^T\boldsymbol{Q}_k\tilde{\boldsymbol{h}}_k^\dagger+\tau\sigma_b^2=1, \quad (23a)\\ &P_s\mathrm{tr}(\boldsymbol{F}_2\boldsymbol{X})\\ &=\bar{\gamma}_e\left(\sigma_r^2\mathrm{tr}(\overline{\boldsymbol{Y}}_2\boldsymbol{X})+\sum_{k=1}^K\boldsymbol{g}_k^T\boldsymbol{Q}_k\boldsymbol{g}_k^\dagger+\tau\sigma_e^2\right), \quad (23b)\\ &\mathrm{tr}(\overline{\boldsymbol{\Phi}}\boldsymbol{X}) \le \tau P_r, \quad (23c)\\ &\mathrm{tr}\,(\boldsymbol{Q}_k) \le \tau\eta P_s\|\boldsymbol{h}_k\|^2, \forall k, \quad (23d)\\ &\boldsymbol{X}\succeq\boldsymbol{0}, \boldsymbol{Q}_k\succeq\boldsymbol{0}, \forall k, \tau\ge 0. \quad (23e)\end{aligned}$$

Lemma 3.2: The constraints in (23a) and (23b) can be replaced by $\sigma_r^2\mathrm{tr}(\overline{\boldsymbol{Y}}_1\boldsymbol{X})+\sum_{k=1}^K\tilde{\boldsymbol{h}}_k^T\boldsymbol{Q}_k\tilde{\boldsymbol{h}}_k^\dagger+\tau\sigma_b^2 \le 1$ and $P_s\mathrm{tr}(\boldsymbol{F}_2\boldsymbol{X}) \le \bar{\gamma}_e(\sigma_r^2\mathrm{tr}(\overline{\boldsymbol{Y}}_2\boldsymbol{X})+\sum_{k=1}^K\boldsymbol{g}_k^T\boldsymbol{Q}_k\boldsymbol{g}_k^\dagger+\tau\sigma_e^2)$, respectively, where both inequalities will be activated when problem (P1′) obtains its optimum value.

Proof: See [34, Appendix A]. ■

Since problem (P1′.1-RW-SDR) is a standard convex optimization problem and satisfies the Slater's condition, its gap with its dual problem is zero [35]. Now, let λ denote the dual variable associated with the equality constraint in (23a), α associated with the other equality constraint in (23b), β_0 associated with the transmit power constraint for the AF relay in (23c), $\{\beta_k\}$ associated with the transmit power constraints for each H_k in (23d), and ζ associated with τ. Then the Lagrangian of problem (P1′.1-RW-SDR) is given by

$$L(\boldsymbol{\Omega}) = \mathrm{tr}(\boldsymbol{A}\boldsymbol{X})+\sum_{k=1}^K\mathrm{tr}(\boldsymbol{B}_k\boldsymbol{Q}_k)+\zeta\tau+\lambda, \tag{24}$$

where $\boldsymbol{\Omega}$ denotes the set of all primal and dual variables,

$$\boldsymbol{A} = P_s\boldsymbol{F}_1-\lambda\sigma_r^2\overline{\boldsymbol{Y}}_1-\alpha P_s\boldsymbol{F}_2+\alpha\bar{\gamma}_e\sigma_r^2\overline{\boldsymbol{Y}}_2-\beta_0\overline{\boldsymbol{\Phi}}, \tag{25}$$

$$\boldsymbol{B}_k = -\lambda\tilde{\boldsymbol{h}}_k^*\tilde{\boldsymbol{h}}_k^T+\alpha\bar{\gamma}_e\boldsymbol{g}_k^*\boldsymbol{g}_k^T-\beta_k\boldsymbol{I}, \forall k, \tag{26}$$

$$\zeta = -\lambda\sigma_b^2+\alpha\bar{\gamma}_e\sigma_e^2+\beta_0P_r+\sum_{k=1}^K\eta P_s\beta_k\|\boldsymbol{h}_k\|^2. \tag{27}$$

TABLE I
ALGORITHM I FOR $(\mathrm{P1}')$

- **Initialize** $\bar{\gamma}_{e_\mathrm{search}} = 0 : \alpha : \bar{\gamma}_{e\max}$ and $i = 0$
- **Repeat**
  1) **Set** $i = i + 1$;
  2) Given $\bar{\gamma}_e = \bar{\gamma}_{e_\mathrm{search}}(i)$,
     solve $(\mathrm{P1}'.1\text{-RW-SDR})$ and **obtain** $H(\bar{\gamma}_e^{(i)})$.
- **Until** $i = L$, where $L = \lfloor \frac{\bar{\gamma}_{e\max}}{\alpha} \rfloor + 1$ is the length of $\bar{\gamma}_{e_\mathrm{search}}$
- **Set** $\bar{\gamma}_e^* = \bar{\gamma}_{e_\mathrm{search}} \left(\arg\max_i \left\{ \frac{1+H(\bar{\gamma}_e^{(i)})}{1+\bar{\gamma}_e^{(i)}} \right\} \right)$ for $(\mathrm{P1}'.2)$
- Given $\bar{\gamma}_e^*$, **solve** $(\mathrm{P1}'.1\text{-RW-SDR})$ to obtain $(\boldsymbol{X}^*, \{\boldsymbol{Q}_k^*\}, \tau^*)$
  if $\mathrm{rank}(\boldsymbol{X}^*) = 1$, **apply** EVD on $\boldsymbol{X}^*$ such that $\boldsymbol{X}^* = \boldsymbol{w}^* \boldsymbol{w}^{*H}$;
  else if the sufficient condition in (32) is satisfied,
  construct $(\hat{\boldsymbol{X}}^*, \{\hat{\boldsymbol{Q}}_k^*\}, \hat{\tau}^*)$ following (29)-(31) and **set** $\boldsymbol{w}^* = \sqrt{b}\boldsymbol{\xi}$;
  else construct $\hat{\boldsymbol{X}}^*$ using the procedure in [36, Algorithm 1].
  end
  end
- **Recover** $\boldsymbol{W}^* = \mathrm{vec}^{-1}(\boldsymbol{w}^*)$

Proposition 3.1: The optimal solution, $(\boldsymbol{X}^*, \{\boldsymbol{Q}_k^*\}, \tau^*)$, to $(\mathrm{P1}'.1\text{-RW-SDR})$ satisfies the following conditions:

1) $\mathrm{rank}(\boldsymbol{Q}_k) \begin{cases} \geq N_t - 2, & \text{if } \beta_k^* = 0, \\ = 1, & \text{if } \beta_k^* > 0, \end{cases} \forall k;$
2) $\boldsymbol{X}^*$ can be expressed as
$$\boldsymbol{X}^* = \sum_{n=1}^{N_t^2 - r_c} a_n \boldsymbol{\eta}_n \boldsymbol{\eta}_n^H + b\boldsymbol{\xi}\boldsymbol{\xi}^H, \tag{28}$$
where $a_n \geq 0\ \forall n$, $b > 0$, $r_c = \mathrm{rank}(\boldsymbol{C}^*)$ (cf. Equation (88)) and $\boldsymbol{\xi} \in \mathbb{C}^{N_t^2 \times 1}$ is a vector orthogonal to $\boldsymbol{\Xi} = \{\boldsymbol{\eta}_n\}_{n=1}^{N_t^2 - r_c}$, which consists of orthonormal basis for $\mathbf{null}(\boldsymbol{C}^*)$;
3) According to (28), if $\mathrm{rank}(\boldsymbol{X}^*) > 1$, then we have the following sufficient condition to yield an optimal solution of $\boldsymbol{X}$ with rank-one:
$$\hat{\boldsymbol{X}}^* = b\boldsymbol{\xi}\boldsymbol{\xi}^H, \tag{29}$$
$$\hat{\boldsymbol{Q}}_k^* = \boldsymbol{Q}_k^*, \forall k, \tag{30}$$
$$\hat{\tau}^* = \tau^* + \Delta\tau, \tag{31}$$
is also optimal to problem $(\mathrm{P1}'.1\text{-RW-SDR})$, if there exists $\Delta\tau \geq 0$ such that
$$\left[\sum_{n=1}^{N_t^2 - r_c} a_n \mathrm{tr}\left(\boldsymbol{\eta}_n^H \left(\frac{\sigma_r^2 \overline{\boldsymbol{Y}}_2}{\sigma_e^2} - \frac{P_s \boldsymbol{F}_2}{\gamma_e \sigma_e^2} \right) \boldsymbol{\eta}_n \right) \right]^+ \leq \Delta\tau \leq \frac{\sigma_r^2}{\sigma_b^2} \sum_{n=1}^{N_t^2 - r_c} a_n \mathrm{tr}\left(\boldsymbol{\eta}_n^H \overline{\boldsymbol{Y}}_1 \boldsymbol{\eta}_n \right). \tag{32}$$

Proof: See Appendix A. ■

Note from Proposition 3.1 that if $\mathrm{rank}(\boldsymbol{X}^*) = 1$, then the optimal $\boldsymbol{w}^*$ to $(\mathrm{P1}'.1\text{-RW})$ can be found directly from the eigenvalue decomposition (EVD) of $\overline{\boldsymbol{X}}^*$, where $\overline{\boldsymbol{X}}^* = \boldsymbol{X}^*/\tau^*$. Namely, the upper-bound optimum value obtained by solving $(\mathrm{P1}'.1\text{-RW-SDR})$ is tight in this case; otherwise, $(\boldsymbol{X}^*, \{\boldsymbol{Q}_k^*\}, \tau^*)$ only serves as an upper-bound solution.

Now, we show that this upper-bound is always achievable by a rank-one $\boldsymbol{X}^*$. When $\mathrm{rank}(\boldsymbol{X}^*) > 1$, firstly, we check whether the sufficient condition proposed in (32) is satisfied. If it is met, then a direct reconstruction of $(\hat{\boldsymbol{X}}^*, \{\hat{\boldsymbol{Q}}_k^*\}, \hat{\tau}^*)$ with $\mathrm{rank}(\hat{\boldsymbol{X}}^*) = 1$ follows according to (29)–(31); otherwise, assume that any optimal solution to problem $(\mathrm{P1}'.1\text{-RW-SDR})$ has no zero component, i.e., $(\boldsymbol{X}^* \neq \boldsymbol{0}, \{\boldsymbol{Q}_k^* \neq \boldsymbol{0}\}, \tau^* \neq 0)$. In addition, the number of optimization variables and the number of shaping constraints are denoted by L and M, respectively. Since $L = K + 2$ and $M = K + 3$ for $(\mathrm{P1}'.1\text{-RW-SDR})$, we have $M \leq L + 2$ satisfied. Thus, according to [36, Proposition 3.5], $(\mathrm{P1}'.1\text{-RW-SDR})$ has an optimal solution of $\hat{\boldsymbol{X}}^*$ that is rank-one. Also, the detailed rank reduction procedure based on an arbitrary-rank solution has been given in [36, Algorithm 1]. Algorithm I for solving $(\mathrm{P1}')$ is shown in Table I.

C. Suboptimal Solutions to $(\mathrm{P1}'.1)$

1) Optimal Solution Structure Based Scheme: We propose a relay beamforming design for $(\mathrm{P1}'.1)$ based on the optimal structure of $\boldsymbol{W}$ [37, Theorem 3.1]. First, define $\boldsymbol{H}_1 \triangleq [\tilde{\boldsymbol{h}}_0\ \boldsymbol{g}_0]$ and $\boldsymbol{H}_2 \triangleq [\boldsymbol{h}_0\ \boldsymbol{g}_0]$. Then express the truncated singular-value decomposition (SVD) of $\boldsymbol{H}_1$ and $\boldsymbol{H}_2$, respectively, as
$$\boldsymbol{H}_1 = \boldsymbol{U}_1 \boldsymbol{\Sigma}_1 \boldsymbol{V}_1^H, \tag{33}$$
$$\boldsymbol{H}_2 = \boldsymbol{U}_2 \boldsymbol{\Sigma}_2 \boldsymbol{V}_2^H. \tag{34}$$

Lemma 3.3: The optimal relay beamforming matrix $\boldsymbol{W}$ for problem $(\mathrm{P1}'.1)$ is of the form:
$$\boldsymbol{W} = \boldsymbol{U}_1^\dagger \boldsymbol{B} \boldsymbol{U}_2^H + \boldsymbol{U}_1^\dagger \boldsymbol{C} (\boldsymbol{U}_2^\perp)^H, \tag{35}$$
where $\boldsymbol{B} \in \mathbb{C}^{2\times 2}$ and $\boldsymbol{C} \in \mathbb{C}^{2\times(N_t-2)}$ are two unknown matrices, and $\boldsymbol{U}_1^\perp, \boldsymbol{U}_2^\perp \in \mathbb{C}^{N_t \times (N_t-2)}$ satisfy $\boldsymbol{U}_1^\perp (\boldsymbol{U}_1^\perp)^H = \boldsymbol{I} - \boldsymbol{U}_1 \boldsymbol{U}_1^H$, $\boldsymbol{U}_2^\perp (\boldsymbol{U}_2^\perp)^H = \boldsymbol{I} - \boldsymbol{U}_2 \boldsymbol{U}_2^H$, respectively.

Proof: See Appendix B. ■

Denote $\boldsymbol{U}_1^H \tilde{\boldsymbol{h}}_0$, $\boldsymbol{U}_2^H \boldsymbol{h}_0$, $\boldsymbol{U}_1^H \boldsymbol{g}_0$ by $\bar{\tilde{\boldsymbol{h}}}_0$, $\bar{\boldsymbol{h}}_0$, $\bar{\boldsymbol{g}}_0$, respectively. We thus simplify $|\tilde{\boldsymbol{h}}_0^T \boldsymbol{W} \boldsymbol{h}_0|^2$ and $|\boldsymbol{g}_0^T \boldsymbol{W} \boldsymbol{h}_0|^2$ as $|\bar{\tilde{\boldsymbol{h}}}_0^T \boldsymbol{B} \bar{\boldsymbol{h}}_0|^2$ and $|\bar{\boldsymbol{g}}_0^T \boldsymbol{B} \bar{\boldsymbol{h}}_0|^2$, respectively. Since $\boldsymbol{C}$ has $2(N_t - 2)$ complex variables, we devise a suboptimal design for $\boldsymbol{C}$ to reduce the size of variables by $(N_t - 2)$. Specifically, let $\boldsymbol{C} = \boldsymbol{u}'^\perp \boldsymbol{v}^T$, where $\boldsymbol{u}' = \bar{\tilde{\boldsymbol{h}}}_0^\dagger / \|\bar{\tilde{\boldsymbol{h}}}_0\|$ such that $\boldsymbol{u}'^\perp \boldsymbol{u}'^{\perp H} = \boldsymbol{I} - \boldsymbol{u}'\boldsymbol{u}'^H$. Hence, $\tilde{\boldsymbol{h}}_0^T \boldsymbol{W} \boldsymbol{W}^H \tilde{\boldsymbol{h}}_0^\dagger$, $\boldsymbol{g}_0^T \boldsymbol{W} \boldsymbol{W}^H \boldsymbol{g}_0^\dagger$ and (5) can be reduced to $\|\boldsymbol{B}^H \bar{\tilde{\boldsymbol{h}}}_0^\dagger\|^2$, $\|\boldsymbol{B}^H \bar{\boldsymbol{g}}_0^\dagger\|^2 + |\boldsymbol{v}^\dagger \boldsymbol{u}'^{\perp H} \bar{\boldsymbol{g}}_0^\dagger|^2$ and $P_s \|\boldsymbol{B}\bar{\boldsymbol{h}}_0\|^2 + \sigma_r^2 \mathrm{tr}(\boldsymbol{B}^H \boldsymbol{B}) + \sigma_r^2 \|\boldsymbol{v}\|^2$, respectively. Then define $\boldsymbol{b} = \mathrm{vec}(\boldsymbol{B})$, $\bar{\boldsymbol{f}}_1 = \mathrm{vec}(\bar{\tilde{\boldsymbol{h}}}_0 \bar{\boldsymbol{h}}_0^T)$, $\bar{\boldsymbol{f}}_2 = \mathrm{vec}(\bar{\boldsymbol{g}}_0 \bar{\boldsymbol{h}}_0^T)$, $\boldsymbol{Y}_1' = \bar{\tilde{\boldsymbol{h}}}_0^T \otimes \boldsymbol{I}$, $\boldsymbol{Y}_2' = \bar{\boldsymbol{g}}_0^T \otimes \boldsymbol{I}$, and $\boldsymbol{\Phi}' = (\boldsymbol{I} \otimes \boldsymbol{\Theta}'^T)^{1/2}$ with $\boldsymbol{\Theta}' = P_s \bar{\boldsymbol{h}}_0 \bar{\boldsymbol{h}}_0^H + \sigma_r^2 \boldsymbol{I}$; $\boldsymbol{Z} = \boldsymbol{b}\boldsymbol{b}^H$, $\boldsymbol{V} = \boldsymbol{v}\boldsymbol{v}^H$, $\overline{\boldsymbol{F}}_1 = \bar{\boldsymbol{f}}_1^\dagger \bar{\boldsymbol{f}}_1^T$, $\overline{\boldsymbol{F}}_2 = \bar{\boldsymbol{f}}_2^\dagger \bar{\boldsymbol{f}}_2^T$, $\overline{\boldsymbol{Y}}_1' = \boldsymbol{Y}_1'^H \boldsymbol{Y}_1'$, $\overline{\boldsymbol{Y}}_2' = \boldsymbol{Y}_2'^H \boldsymbol{Y}_2'$, and $\overline{\boldsymbol{\Phi}}' = \boldsymbol{\Phi}'^H \boldsymbol{\Phi}'$. The suboptimal design for problem $(\mathrm{P1}'.1)$ by ignoring the rank constraints on $\boldsymbol{Z}$ and $\boldsymbol{V}$ is thus given by

$$(\mathrm{P1}'.1\text{-sub1-SDR}) : \max_{\boldsymbol{Z}, \boldsymbol{V}, \{\boldsymbol{Q}_k\}, \tau} \quad P_s \mathrm{tr}(\overline{\boldsymbol{F}}_1 \boldsymbol{Z})$$
$$\text{s.t. } \sigma_r^2 \mathrm{tr}(\overline{\boldsymbol{Y}}_1' \boldsymbol{Z}) + \sum_{k=1}^K \tilde{\boldsymbol{h}}_k^T \boldsymbol{Q}_k \tilde{\boldsymbol{h}}_k^\dagger + \tau\sigma_b^2 = 1, \tag{36a}$$
$$P_s \mathrm{tr}(\overline{\boldsymbol{F}}_2 \boldsymbol{Z}) \leq \bar{\gamma}_e \left(\sigma_r^2 \left(\mathrm{tr}(\overline{\boldsymbol{Y}}_2' \boldsymbol{Z}) + |\bar{\boldsymbol{g}}_0^T \boldsymbol{u}'^\perp|^2 \mathrm{tr}(\boldsymbol{V}) \right) + \sum_{k=1}^K \boldsymbol{g}_k^T \boldsymbol{Q}_k \boldsymbol{g}_k^\dagger + \tau\sigma_e^2 \right), \tag{36b}$$
$$\mathrm{tr}(\overline{\boldsymbol{\Phi}}' \boldsymbol{Z}) + \sigma_r^2 \mathrm{tr}(\boldsymbol{Z}) + \sigma_r^2 \mathrm{tr}(\boldsymbol{V}) \leq \tau P_r, \tag{36c}$$
$$\mathrm{tr}(\boldsymbol{Q}_k) \leq \tau\eta P_s \|\boldsymbol{h}_k\|^2, \forall k, \tag{36d}$$
$$\tau \geq 0, \boldsymbol{Q}_k \succeq \boldsymbol{0}, \forall k, \boldsymbol{Z} \succeq \boldsymbol{0}, \boldsymbol{V} \succeq \boldsymbol{0}. \tag{36e}$$

Remark 3.1: The variables in (P1′.1-sub1-SDR), i.e., $\boldsymbol{Z} \in \mathbb{C}^{4\times 4}$, $\boldsymbol{V} \in \mathbb{C}^{(N_t-2)\times(N_t-2)}$, are of much reduced size. Further, the reconstruction of $\boldsymbol{v}^*$ from $\boldsymbol{V}$ can be briefly explained as follows. Given the Lagrangian of (P1′.1-sub1-SDR), the KKT conditions with respect to (w.r.t.) $\boldsymbol{V}^*$ are given by

$$(\alpha^*\bar{\gamma}_e|\bar{\boldsymbol{g}}_0^T\boldsymbol{u}'^{\perp}|^2 - \beta_0^*\sigma_r^2)\boldsymbol{I} + \boldsymbol{U}^* = 0, \tag{37}$$

$$\boldsymbol{U}^*\boldsymbol{V}^* = 0. \tag{38}$$

Post-multiplying (37) with $\boldsymbol{V}^*$, we have $(\alpha^*\bar{\gamma}_e|\bar{\boldsymbol{g}}_0^T\boldsymbol{u}'^{\perp}|^2 - \beta_0^*\sigma_r^2)\boldsymbol{V}^* = 0$. As a result, if $\frac{\alpha^*}{\beta_0^*} \neq \frac{\sigma_r^2}{\bar{\gamma}_e|\bar{\boldsymbol{g}}_0^T\boldsymbol{u}'^{\perp}|^2}$, $\boldsymbol{V}^* = \boldsymbol{0}$; otherwise $\boldsymbol{V}^* = \boldsymbol{v}^*\boldsymbol{v}^{*H}$, with $\boldsymbol{v}^* = \sqrt{\mathrm{tr}(\boldsymbol{V}^*)}\boldsymbol{v}_0$, where $\boldsymbol{v}_0 \in \mathbb{C}^{(N_t-2)\times 1}$ is an arbitrary vector with unit norm. With $\boldsymbol{V}$ solved, (P1′.1-sub1-SDR) reduces to a problem with similar structure as (P1′.1-RW-SDR), and the proof for existence of a rank-one $\boldsymbol{Z}$ can be referred to Proposition 3.1.

2) Zero-forcing: We propose a low-complexity ZF scheme for (P1′.1), in which the jamming signal places a null at Bob, and then a semi-closed form solution for $\boldsymbol{W}$ is derived. In line with the principle of ZF jamming [17], the jamming signal $\boldsymbol{n}_k$ is designed as $\boldsymbol{n}_k = \tilde{\boldsymbol{V}}_k\tilde{\boldsymbol{n}}_k$ such that $\boldsymbol{I} - \frac{\tilde{\boldsymbol{h}}_k^{\dagger}\tilde{\boldsymbol{h}}_k^T}{\|\tilde{\boldsymbol{h}}_k\|^2} = \tilde{\boldsymbol{V}}_k\tilde{\boldsymbol{V}}_k^H$, and $\tilde{\boldsymbol{n}}_k \in \mathbb{C}^{(N_t-1)\times 1}$ is an arbitrary random vector, $\tilde{\boldsymbol{n}}_k \sim \mathcal{CN}(\boldsymbol{0}, \tilde{\boldsymbol{Q}}_k)$, $k = 1, \ldots, K$. Thus, given any $\boldsymbol{W}$, $\tilde{\boldsymbol{n}}_k$'s can be optimized to maximize the effect of jamming at Eve by $\max_{\tilde{\boldsymbol{Q}}_k}\sum_{k=1}^K \boldsymbol{g}_k^T\tilde{\boldsymbol{V}}_k\tilde{\boldsymbol{Q}}_k\tilde{\boldsymbol{V}}_k^H\boldsymbol{g}_k^{\dagger}$, which gives $\tilde{\boldsymbol{Q}}_k^* = \zeta_k^2\tilde{\boldsymbol{g}}_k^{\dagger}\tilde{\boldsymbol{g}}_k^T$, where $\tilde{\boldsymbol{g}}_k = \tilde{\boldsymbol{V}}_k^T\boldsymbol{g}_k$, and $\zeta_k = \sqrt{\eta P_s}\|\boldsymbol{h}_k\|/\|\tilde{\boldsymbol{g}}_k\|$ is determined by (23d), $\forall k$. As such, $\sum_{k=1}^K \boldsymbol{g}_k^T\tilde{\boldsymbol{V}}_k\tilde{\boldsymbol{Q}}_k^*\tilde{\boldsymbol{V}}_k^H\boldsymbol{g}_k^{\dagger}$ turns out to be $\sum_{k=1}^K \eta P_s\|\boldsymbol{h}_k\|^2\|\tilde{\boldsymbol{g}}_k\|^2$, which is denoted by q.

With fixed q, (P1′.1-RW-SDR) can be recast as

$$\begin{aligned}
&(\mathrm{P1'.1\text{-}sub2\text{-}SDR}): \max_{\boldsymbol{X},\tau}\ P_s\mathrm{tr}(\boldsymbol{F}_1\boldsymbol{X})\\
&\mathrm{s.t.}\ \sigma_r^2\mathrm{tr}(\overline{\boldsymbol{Y}}_1\boldsymbol{X}) + \tau\sigma_b^2 = 1, && (39a)\\
&P_s\mathrm{tr}(\boldsymbol{F}_2\boldsymbol{X}) \le \bar{\gamma}_e\left(\sigma_r^2\mathrm{tr}(\overline{\boldsymbol{Y}}_2\boldsymbol{X}) + \tau q + \tau\sigma_e^2\right), && (39b)\\
&\mathrm{tr}(\overline{\boldsymbol{\Phi}}\boldsymbol{X}) \le \tau P_r, && (39c)\\
&\boldsymbol{X} \succeq \boldsymbol{0}, \tau \ge 0. && (39d)
\end{aligned}$$

Proposition 3.2: (P1′.1-sub2-SDR) must yield a rank-one solution, i.e., $\boldsymbol{X}^* = \boldsymbol{w}\boldsymbol{w}^*$, such that $\boldsymbol{w}^* = \mu\boldsymbol{\nu}_{\max}(\boldsymbol{Z}^*)$, and

$$\boldsymbol{Z}^* = P_s\boldsymbol{F}_1 - \lambda^*\sigma_r^2\overline{\boldsymbol{Y}}_1 - \alpha^*P_s\boldsymbol{F}_2 + \alpha^*\bar{\gamma}_e\sigma_r^2\overline{\boldsymbol{Y}}_2 - \beta_0^*\overline{\boldsymbol{\Phi}}, \tag{40}$$

where $\boldsymbol{\nu}_{\max}(\cdot)$ represents the eigenvector corresponding to the largest eigenvalue of the associated matrix, and $\mu = \sqrt{\frac{P_r}{\mathrm{tr}(\overline{\boldsymbol{\Phi}})\boldsymbol{\nu}_{\max}(\boldsymbol{Z}^*)\boldsymbol{\nu}_{\max}^H(\boldsymbol{Z}^*)}}$. Also, λ^*, α^* and β_0^* are the optimal dual variables associated with (39a)–(39c), respectively.

Proof: See Appendix C. ■

The only problem in Proposition 3.2 is the dual problem of (P1′.1-sub2-SDR), which admits a much simpler structure to solve than the primal one.

IV. Joint AN-AF Beamforming With Imperfect CSI

A. Problem Formulation for Imperfect CSI

We use a deterministic spherical model [25], [26] to characterize the resulting CSIs' uncertainties such that

$$\mathcal{G}_0 = \{\boldsymbol{g}_0|\boldsymbol{g}_0 = \hat{\boldsymbol{g}}_0 + \Delta\boldsymbol{g}_0, \Delta\boldsymbol{g}_0^H\boldsymbol{W}_0\Delta\boldsymbol{g}_0 \le 1\}, \tag{41a}$$

$$\mathcal{G}_k = \{\boldsymbol{g}_k|\boldsymbol{g}_k = \hat{\boldsymbol{g}}_k + \Delta\boldsymbol{g}_k, \Delta\boldsymbol{g}_k^H\boldsymbol{W}_k\Delta\boldsymbol{g}_k \le 1\}, \forall k, \tag{41b}$$

$$\tilde{\mathcal{H}}_0 = \{\tilde{\boldsymbol{h}}_0|\tilde{\boldsymbol{h}}_0 = \hat{\tilde{\boldsymbol{h}}}_0 + \Delta\tilde{\boldsymbol{h}}_0, \Delta\tilde{\boldsymbol{h}}_0^H\boldsymbol{W}_0'\Delta\tilde{\boldsymbol{h}}_0 \le 1\}, \tag{41c}$$

$$\tilde{\mathcal{H}}_k = \{\tilde{\boldsymbol{h}}_k|\tilde{\boldsymbol{h}}_k = \hat{\tilde{\boldsymbol{h}}}_k + \Delta\tilde{\boldsymbol{h}}_k, \Delta\tilde{\boldsymbol{h}}_k^H\boldsymbol{W}_k''\Delta\tilde{\boldsymbol{h}}_k \le 1\}, \forall k, \tag{41d}$$

$$\mathcal{H}_k = \{\boldsymbol{h}_k|\boldsymbol{h}_k = \hat{\boldsymbol{h}}_k + \Delta\boldsymbol{h}_k, \Delta\boldsymbol{h}_k^H\boldsymbol{W}_k'\Delta\boldsymbol{h}_k \le 1\}, \forall k, \tag{41e}$$

where $\hat{\boldsymbol{g}}_0$, $\hat{\boldsymbol{g}}_k$'s, $\hat{\tilde{\boldsymbol{h}}}_0$, $\hat{\tilde{\boldsymbol{h}}}_k$'s and $\hat{\boldsymbol{h}}_k$'s are the estimates of the corresponding channels; $\Delta\boldsymbol{g}_0$, $\Delta\boldsymbol{g}_k$'s, $\Delta\tilde{\boldsymbol{h}}_0$, $\Delta\tilde{\boldsymbol{h}}_k$'s and $\Delta\boldsymbol{h}_k$'s are their respective channel errors; the matrices $\boldsymbol{W}_0$, $\boldsymbol{W}_k$'s, $\boldsymbol{W}_0'$, $\boldsymbol{W}_k''$'s and $\boldsymbol{W}_k'$'s determine the shape of each error region. Without loss of generality (w.l.o.g.), we set $\boldsymbol{W}_0 = \boldsymbol{I}/\epsilon_0$, $\boldsymbol{W}_0' = \boldsymbol{I}/\epsilon_0'$, $\boldsymbol{W}_k = \boldsymbol{I}/\epsilon_k$, $\boldsymbol{W}_k' = \boldsymbol{I}/\epsilon_k'$ and $\boldsymbol{W}_k'' = \boldsymbol{I}/\epsilon_k''$ for simplicity, where ϵ_0, ϵ_0', ϵ_k, ϵ_k', and ϵ_k'' represent the respective size of the bounded error regions, $k = 1, \ldots, K$.

Accordingly, we denote the robust counterpart for (P1′) as

$$\begin{aligned}
(\mathrm{P2'}):\quad &\max_{\{\boldsymbol{Q}_k\},\boldsymbol{W}}\ \min_{\substack{\tilde{\boldsymbol{h}}_0\in\tilde{\mathcal{H}}_0,\tilde{\boldsymbol{h}}_k\in\tilde{\mathcal{H}}_k,\forall k\\ \boldsymbol{g}_0\in\boldsymbol{G}_0,\tilde{\boldsymbol{g}}_k\in\tilde{\mathcal{G}}_k,\forall k}} \bar{F}(\{\boldsymbol{Q}_k\},\boldsymbol{W})\\
\mathrm{s.t.}\quad &\mathrm{tr}\left(\boldsymbol{W}\left(P_s\boldsymbol{h}_0\boldsymbol{h}_0^H + \sigma_r^2\boldsymbol{I}\right)\boldsymbol{W}^H\right) \le P_r, && (42a)\\
&\mathrm{tr}(\boldsymbol{Q}_k) \le \eta P_s \min_{\boldsymbol{h}_k\in\mathcal{H}_k,\forall k}\|\boldsymbol{h}_k\|^2, \forall k, && (42b)\\
&\boldsymbol{Q}_k \succeq \boldsymbol{0}, \forall k. && (42c)
\end{aligned}$$

An equivalent robust reformulation of (P1′.2) is given by

$$(\mathrm{P2'.2}): \max_{\bar{\gamma}_e>0}\frac{1+\hat{H}(\bar{\gamma}_e)}{1+\hat{F}(\bar{\gamma}_e)}, \tag{43}$$

where $\hat{F}(\bar{\gamma}_e) = \gamma_e$ and $\hat{H}(\bar{\gamma}_e)$ denotes the optimal value of problem (P2′.1) that is given by

$$\begin{aligned}
&(\mathrm{P2'.1}):\\
&\max_{\boldsymbol{X},\{\boldsymbol{Q}_k\}}\ \min_{\substack{\tilde{\boldsymbol{h}}_k\in\tilde{\mathcal{H}}_k,\forall k\\ \tilde{\boldsymbol{h}}_0\in\tilde{\mathcal{H}}_0}} \frac{P_s\mathrm{tr}(\boldsymbol{F}_1\boldsymbol{X})}{\sigma_r^2\mathrm{tr}(\overline{\boldsymbol{Y}}_1\boldsymbol{X}) + \sum_{k=1}^K\tilde{\boldsymbol{h}}_k^T\boldsymbol{Q}_k\tilde{\boldsymbol{h}}_k^{\dagger} + \sigma_b^2}\\
&\mathrm{s.t.}\ \max_{\substack{\boldsymbol{g}_k\in\tilde{\mathcal{G}}_k,\forall k\\ \boldsymbol{g}_0\in\mathcal{G}_0}} \frac{P_s\mathrm{tr}(\boldsymbol{F}_2\boldsymbol{X})}{\sigma_r^2\mathrm{tr}(\overline{\boldsymbol{Y}}_2\boldsymbol{X}) + \sum_{k=1}^K\boldsymbol{g}_k^T\boldsymbol{Q}_k\boldsymbol{g}_k^{\dagger} + \sigma_e^2} \le \bar{\gamma}_e, && (44a)\\
&\mathrm{tr}(\overline{\boldsymbol{\Phi}}\boldsymbol{X}) \le P_r, && (44b)\\
&\mathrm{tr}\left(\boldsymbol{Q}_k\right) \le \eta P_s \min_{\boldsymbol{h}_k\in\mathcal{H}_k,\forall k}\|\boldsymbol{h}_k\|^2, \forall k, && (44c)\\
&\mathrm{rank}(\boldsymbol{X}) = 1, && (44d)\\
&\boldsymbol{X} \succeq \boldsymbol{0}, \boldsymbol{Q}_k \succeq \boldsymbol{0}, \forall k. && (44e)
\end{aligned}$$

As stated in Lemma 3.1, similarly, (P2′) can be proved to have the same optimal value as (P2′.2) and the same optimal solution as (P2′.1) when $\bar{\gamma}_e$ takes its optimal value. As a result, (P2′) can be solved in a two-stage fashion as well. Specifically, given any $\bar{\gamma}_e$, we first solve (P2′.1) to obtain $\hat{H}(\bar{\gamma}_e)$ and then search for the optimal $\bar{\gamma}_e$ to (P2′.2).

B. Solutions to $(\mathrm{P2}'.1)$

By ignoring (44d), $(\mathrm{P2}'.1)$ is recast as

$$\begin{aligned}&(\mathrm{P2}'.1\text{-RW-SDR-Eqv}):\\&\max_{\boldsymbol{X},\{\boldsymbol{Q}_k\}}\ \min_{\substack{\tilde{\boldsymbol{h}}_k\in\tilde{\mathcal{H}}_k,\forall k\\ \tilde{\boldsymbol{h}}_0\in\tilde{\mathcal{H}}_0}}\ \frac{P_s\mathrm{tr}(\boldsymbol{F}_1\boldsymbol{X})}{\sigma_r^2\mathrm{tr}(\overline{\boldsymbol{Y}}_1\boldsymbol{X})+\sum_{k=1}^K\tilde{\boldsymbol{h}}_k^T\boldsymbol{Q}_k\tilde{\boldsymbol{h}}_k^\dagger+\sigma_b^2}\\&\mathtt{s.t.}(44\mathrm{a})\text{-}(44\mathrm{c}),(44\mathrm{e}).\end{aligned}\tag{45a}$$

It is worth noting that due to the rank-one relaxation of $(\mathrm{P2}'.1\text{-RW-SDR-Eqv})$, solution provided by $(\mathrm{P2}'.1\text{-RW-SDR-Eqv})$ in general yields an upper-bound for $\hat{H}(\bar{\gamma}_e)$, which may not be achievable. However, in the sequel we insist on solving $(\mathrm{P2}'.1\text{-RW-SDR-Eqv})$ that is regarded as an upper-bound benchmark for our proposed problem detailed later in this subsection.

1) Solutions to $(\mathrm{P2}'.1\text{-RW-SDR-Eqv})$*:* To make the "max-min" objective function of (45) tractable, we first rewrite (45) by the equivalent epigraph formulation as

$$\begin{aligned}&(\mathrm{P2}'.1\text{-RW-SDR-Eqv}):\\&\max_{\boldsymbol{X},\{\boldsymbol{Q}_k\},\delta}\ \delta\\&\mathtt{s.t.}\ \min_{\substack{\tilde{\boldsymbol{h}}_k\in\tilde{\mathcal{H}}_k,\forall k\\ \tilde{\boldsymbol{h}}_0\in\tilde{\mathcal{H}}_0}}\ \frac{P_s\mathrm{tr}(\boldsymbol{F}_1\boldsymbol{X})}{\sigma_r^2\mathrm{tr}(\overline{\boldsymbol{Y}}_1\boldsymbol{X})+\sum_{k=1}^K\tilde{\boldsymbol{h}}_k^T\boldsymbol{Q}_k\tilde{\boldsymbol{h}}_k^\dagger+\sigma_b^2}\geq\delta,\end{aligned}\tag{46a}$$

$$(44\mathrm{a})\text{-}(44\mathrm{c}),(44\mathrm{e}).\tag{46b}$$

As there are potentially infinite number of constraints in (46a), (44a), and (44c), they are semi-indefinite and thus intractable. In the following, we equivalently transform these constraints to tractable ones using *S-Procedure* and a generalized *S-Procedure* given in Lemmas 4.1 and 4.2, respectively.

Lemma 4.1 (S-Procedure [35]): Let $f_m(\boldsymbol{x})$, $m=1,2$ be defined as

$$f_m(\boldsymbol{x})=\boldsymbol{x}^H\boldsymbol{A}_m\boldsymbol{x}+2\Re\{\boldsymbol{b}_m^H\boldsymbol{x}\}+c_m,\tag{47}$$

where $\boldsymbol{A}_m=\boldsymbol{A}_m^H\in\mathbb{C}^{N\times N}$, $\boldsymbol{b}_m\in\mathbb{C}^{N\times 1}$ and $c_m\in\mathbb{R}$, and $\Re$ gives the real part of the input entity. Then the implication $f_1(\boldsymbol{x})\geq 0\Rightarrow f_2(\boldsymbol{x})\geq 0$ holds if and only if there exists $\delta\geq 0$ such that

$$\begin{bmatrix}\boldsymbol{A}_2 & \boldsymbol{b}_2\\ \boldsymbol{b}_2^H & c_2\end{bmatrix}-\delta\begin{bmatrix}\boldsymbol{A}_1 & \boldsymbol{b}_1\\ \boldsymbol{b}_1^H & c_1\end{bmatrix}\succeq\boldsymbol{0},\tag{48}$$

provided there exists a point $\hat{\boldsymbol{x}}$ such that $f_m(\hat{\boldsymbol{x}})>0$, $m=1,2$.

Lemma 4.2 ([38, Theorem 3.5]): The robust block quadratic matrix inequality (QMI),

$$\begin{bmatrix}\boldsymbol{H} & \boldsymbol{F}+\boldsymbol{G}\boldsymbol{X}\\ (\boldsymbol{F}+\boldsymbol{G}\boldsymbol{X})^H & \boldsymbol{C}+\boldsymbol{X}^H\boldsymbol{B}+\boldsymbol{B}^H\boldsymbol{X}+\boldsymbol{X}^H\boldsymbol{A}\boldsymbol{X}\end{bmatrix}\succeq\boldsymbol{0},\quad\text{for all }\boldsymbol{I}-\boldsymbol{X}^H\boldsymbol{D}\boldsymbol{X}\succeq\boldsymbol{0},\tag{49}$$

is equivalent to

$$\exists t\geq 0,\text{such that}\begin{bmatrix}\boldsymbol{H} & \boldsymbol{F} & \boldsymbol{G}\\ \boldsymbol{F}^H & \boldsymbol{C} & \boldsymbol{B}^H\\ \boldsymbol{G}^H & \boldsymbol{B} & \boldsymbol{A}\end{bmatrix}-t\begin{bmatrix}\boldsymbol{0} & \boldsymbol{0} & \boldsymbol{0}\\ \boldsymbol{0} & \boldsymbol{I} & \boldsymbol{0}\\ \boldsymbol{0} & \boldsymbol{0} & -\boldsymbol{D}\end{bmatrix}\succeq\boldsymbol{0}.\tag{50}$$

First, by rearranging terms, (46a) can be equivalently transformed into the following linear form:

$$\min_{\substack{\tilde{\boldsymbol{h}}_k\in\tilde{\mathcal{H}}_k,\forall k\\ \tilde{\boldsymbol{h}}_0\in\tilde{\mathcal{H}}_0}}P_s\mathrm{tr}(\boldsymbol{F}_1\boldsymbol{X})-\delta\sigma_r^2\mathrm{tr}(\overline{\boldsymbol{Y}}_1\boldsymbol{X})-\delta\sum_{k=1}^K\tilde{\boldsymbol{h}}_k^T\boldsymbol{Q}_k\tilde{\boldsymbol{h}}_k^\dagger-\delta\sigma_b^2\geq 0.\tag{51}$$

Recalling the following matrix equalities in line with our definition of $\mathrm{vec}(\cdot)$ operation:

$$\mathrm{tr}(\boldsymbol{A}\boldsymbol{B}^T)=\mathrm{vec}^T(\boldsymbol{A})\mathrm{vec}(\boldsymbol{B}),\tag{52}$$

$$\mathrm{vec}(\boldsymbol{A}\boldsymbol{X}\boldsymbol{B})=(\boldsymbol{A}\otimes\boldsymbol{B}^T)\mathrm{vec}(\boldsymbol{X}),\tag{53}$$

$$(\boldsymbol{A}\otimes\boldsymbol{B})^T=\boldsymbol{A}^T\otimes\boldsymbol{B}^T,\tag{54}$$

it follows that

$$\mathrm{tr}(\boldsymbol{F}_1\boldsymbol{X})=\tilde{\boldsymbol{h}}^T(\boldsymbol{h}_0\otimes\boldsymbol{I})X(\boldsymbol{h}_0^H\otimes\boldsymbol{I})\tilde{\boldsymbol{h}}^\dagger,\tag{55}$$

$$\mathrm{tr}(\overline{\boldsymbol{Y}}_1\boldsymbol{X})=\tilde{\boldsymbol{h}}^T(\boldsymbol{I}\otimes\boldsymbol{X})\tilde{\boldsymbol{h}}^\dagger,\tag{56}$$

where $\tilde{\boldsymbol{h}}\in\mathbb{C}^{N_t^3\times 1}=\mathrm{vec}(\tilde{\boldsymbol{h}}_0^T\otimes\boldsymbol{I})$. The equivalent channel model for $\tilde{\boldsymbol{h}}$ is given by $\tilde{\boldsymbol{h}}=\hat{\tilde{\boldsymbol{h}}}+\Delta\tilde{\boldsymbol{h}}$, where $\|\Delta\tilde{\boldsymbol{h}}\|^2\leq N_t\epsilon_0'$ (cf. Equation (41)). By introducing $\boldsymbol{X}''=(\boldsymbol{h}_0\otimes\boldsymbol{I})\boldsymbol{X}(\boldsymbol{h}_0^H\otimes\boldsymbol{I})$ and $\boldsymbol{X}'=\boldsymbol{I}\otimes\boldsymbol{X}$, (51) can thus be recast as

$$\min_{\substack{\tilde{\boldsymbol{h}}_k\in\tilde{\mathcal{H}}_k,\forall k\\ \tilde{\boldsymbol{h}}_0\in\tilde{\mathcal{H}}_0}}\Delta\tilde{\boldsymbol{h}}^T(P_s\boldsymbol{X}''-\delta\sigma_r^2\boldsymbol{X}')\Delta\tilde{\boldsymbol{h}}^\dagger+2\Re\{\Delta\tilde{\boldsymbol{h}}^T(P_s\boldsymbol{X}''-\delta\sigma_r^2\boldsymbol{X}')\hat{\tilde{\boldsymbol{h}}}^\dagger\}-\delta\sum_{k=1}^K\tilde{\boldsymbol{h}}_k^T\boldsymbol{Q}_k\tilde{\boldsymbol{h}}_k^\dagger-\delta\sigma_b^2\geq 0.\tag{57}$$

Hence, according to Lemma 4.1, the implication $\|\Delta\tilde{\boldsymbol{h}}\|^2\leq N_t\epsilon_0'\Rightarrow$ (57) holds if and only if there exists $w^{(0)}\geq 0$ such that the following LMI holds:

$$\begin{bmatrix}\boldsymbol{H}_1 & \boldsymbol{F}_1\\ \boldsymbol{F}_1^H & c_1\end{bmatrix}\succeq\boldsymbol{0},\tag{58}$$

where $\boldsymbol{H}_1=P_s\boldsymbol{X}''-\delta\sigma_r^2\boldsymbol{X}'+w^{(0)}\boldsymbol{I}$, $\boldsymbol{F}_1=(P_s\boldsymbol{X}''-\delta\sigma_r^2\boldsymbol{X}')\hat{\tilde{\boldsymbol{h}}}^\dagger$ and $c_1=\hat{\tilde{\boldsymbol{h}}}^T(P_s\boldsymbol{X}''-\delta\sigma_r^2\boldsymbol{X}')\hat{\tilde{\boldsymbol{h}}}^\dagger-\delta\sum_{k=1}^K\tilde{\boldsymbol{h}}_k^T\boldsymbol{Q}_k\tilde{\boldsymbol{h}}_k^\dagger-\delta\sigma_b^2-w^{(0)}N_t\epsilon_0'$. Now, (46a) has been equivalently reformulated as (58). To further cope with channel uncertainties with regards to $\tilde{\boldsymbol{h}}_k$'s such that (58) holds for $\tilde{\boldsymbol{h}}_k\in\tilde{\mathcal{H}}_k$, $k=1,\ldots,K$, we need the following proposition.

Proposition 4.1: The semi-indefinite constraint of (57) can be equivalently recast as the following block matrix inequality:

$$\begin{bmatrix}\boldsymbol{H}_1^{(K)} & \boldsymbol{F}_1^{(K)} & \boldsymbol{G}_1^{(K)}\\ \boldsymbol{F}_1^{(K)H} & c_1^{(K)} & \boldsymbol{B}_1^{(K)H}\\ \boldsymbol{G}_1^{(K)H} & \boldsymbol{B}_1^{(K)} & \boldsymbol{A}_1^{(K)}\end{bmatrix}-w^{(K)}\begin{bmatrix}\boldsymbol{0} & \boldsymbol{0} & \boldsymbol{0}\\ \boldsymbol{0} & 1 & \boldsymbol{0}\\ \boldsymbol{0} & \boldsymbol{0} & \frac{-\boldsymbol{I}}{\epsilon_K''}\end{bmatrix}\succeq\boldsymbol{0},\tag{59}$$

where $\boldsymbol{H}_1^{(K)}$, $\boldsymbol{F}_1^{(K)}$ and $c_1^{(K)}$ are recursively given by

$$\boldsymbol{H}_1^{(k)}=\begin{cases}\begin{bmatrix}\boldsymbol{A}_1^{(k-1)}+\frac{w^{(k-1)}}{\epsilon_{k-1}''}\boldsymbol{I} & \boldsymbol{G}_1^{(k-1)H}\\ \boldsymbol{G}_1^{(k-1)} & \boldsymbol{H}_1^{(k-1)}\end{bmatrix}, & k>1;\\ P_s\boldsymbol{X}''-\delta\sigma_r^2\boldsymbol{X}'+w^{(0)}\boldsymbol{I}, & k=1,\end{cases}\tag{60}$$

$$\boldsymbol{F}_1^{(k)} = \begin{cases} \begin{bmatrix} \boldsymbol{B}_1^{(k-1)} \\ \boldsymbol{F}_1^{(k-1)} \end{bmatrix}, & k > 1; \\ (P_s\boldsymbol{X}'' - \delta\sigma_r^2\boldsymbol{X}')\hat{\tilde{\boldsymbol{h}}}^\dagger, & k = 1, \end{cases} \tag{61}$$

$c_1^{(k)} = \hat{\tilde{\boldsymbol{h}}}^T(P_s\boldsymbol{X}'' - \delta\sigma_r^2\boldsymbol{X}')\hat{\tilde{\boldsymbol{h}}}^\dagger - \delta\sum_{j=1}^{k}\hat{\tilde{\boldsymbol{h}}}_j^T\boldsymbol{Q}_j\hat{\tilde{\boldsymbol{h}}}_j^\dagger - \delta\sum_{i=k+1}^{K}\tilde{\boldsymbol{h}}_i^T\boldsymbol{Q}_i\tilde{\boldsymbol{h}}_i^\dagger - \delta\sigma_b^2 - w^{(0)}N_t\epsilon_0' - \sum_{l=1}^{k-1}w^{(l)}$, $k = 1,\ldots,K$. In addition, $\boldsymbol{G}_1^{(k)} \in \mathbb{C}^{(N_t^3+(k-1)N_t)\times N_t} = \boldsymbol{0}$, $\boldsymbol{B}_1^{(k)} = -\delta\boldsymbol{Q}_k\hat{\tilde{\boldsymbol{h}}}_k^\dagger$, $\boldsymbol{A}_1^{(k)} = -\delta\boldsymbol{Q}_k$, $k = 1,\ldots,K$, and $\{w^{(k)} \geq 0\}$ denote pertinent auxiliary variables.

Proof: See Appendix D. ■

Next, (44a) is rewritten as

$$\max_{\substack{\boldsymbol{g}_k\in\mathcal{G}_k,\forall k\\ \boldsymbol{g}_0\in\mathcal{G}_0}} \boldsymbol{g}^T(P_s\boldsymbol{X}'' - \bar{\gamma}_e\sigma_r^2\boldsymbol{X}')\boldsymbol{g}^\dagger - \bar{\gamma}_e\sum_{k=1}^{K}\boldsymbol{g}_k^T\boldsymbol{Q}_k\boldsymbol{g}_k^\dagger - \bar{\gamma}_e\sigma_e^2 \leq 0, \tag{62}$$

where $\boldsymbol{g} \in \mathbb{C}^{N_t^2\times 1} = \mathrm{vec}(\boldsymbol{g}_0^T \otimes \boldsymbol{I})$ and the equivalent imperfect channel model is given by $\boldsymbol{g} = \hat{\boldsymbol{g}} + \Delta\boldsymbol{g}$ such that $\|\Delta\boldsymbol{g}\|^2 \leq N_t\epsilon_0$.

Proposition 4.2: The semi-indefinite constraint of (62) is satisfied if and only if there exists $v^{(k)} \geq 0$, $k = 1,\ldots,K$, such that the following block matrix inequality holds:

$$\begin{bmatrix} \boldsymbol{H}_2^{(K)} & \boldsymbol{F}_2^{(K)} & \boldsymbol{G}_2^{(K)} \\ \boldsymbol{F}_2^{(K)H} & c_2^{(K)} & \boldsymbol{B}_2^{(K)H} \\ \boldsymbol{G}_2^{(K)H} & \boldsymbol{B}_2^{(K)} & \boldsymbol{A}_2^{(K)} \end{bmatrix} - v^{(K)}\begin{bmatrix} \boldsymbol{0} & \boldsymbol{0} & \boldsymbol{0} \\ \boldsymbol{0} & 1 & \boldsymbol{0} \\ \boldsymbol{0} & \boldsymbol{0} & \frac{-\boldsymbol{I}}{\epsilon_K} \end{bmatrix} \succeq \boldsymbol{0}, \tag{63}$$

where $\boldsymbol{H}_2^{(K)}$, $\boldsymbol{F}_2^{(K)}$ and $c_2^{(K)}$ are recursively given by

$$\boldsymbol{H}_2^{(k)} = \begin{cases} \begin{bmatrix} \boldsymbol{A}_2^{(k-1)} + \frac{v^{(k-1)}}{\epsilon_{k-1}}\boldsymbol{I} & \boldsymbol{G}_2^{(k-1)H} \\ \boldsymbol{G}_2^{(k-1)} & \boldsymbol{H}_2^{(k-1)} \end{bmatrix}, & k>1; \\ -P_s\boldsymbol{X}'' + \bar{\gamma}_e\sigma_r^2\boldsymbol{X}' + v^{(0)}\boldsymbol{I}, & k = 1, \end{cases} \tag{64}$$

$$\boldsymbol{F}_2^{(k)} = \begin{cases} \begin{bmatrix} \boldsymbol{B}_2^{(k-1)} \\ \boldsymbol{F}_2^{(k-1)} \end{bmatrix}, & k > 1; \\ (-P_s\boldsymbol{X}'' + \bar{\gamma}_e\sigma_r^2\boldsymbol{X}')\hat{\boldsymbol{g}}^\dagger, & k = 1, \end{cases} \tag{65}$$

$$c_2^{(k)} = \hat{\boldsymbol{g}}^T(-P_s\boldsymbol{X}'' + \bar{\gamma}_e\sigma_r^2\boldsymbol{X}')\hat{\boldsymbol{g}}^\dagger + \bar{\gamma}_e\sum_{j=1}^{k}\hat{\boldsymbol{g}}_j^T\boldsymbol{Q}_j\hat{\boldsymbol{g}}_j^\dagger + \bar{\gamma}_e\sum_{i=k+1}^{K}\boldsymbol{g}_i^T\boldsymbol{Q}_i\boldsymbol{g}_i^\dagger + \bar{\gamma}_e\sigma_e^2 - v^{(0)}N_t\epsilon_0 - \sum_{l=1}^{k-1}v^{(l)}, \tag{66}$$

$k = 1,\ldots,K$. Also, $\boldsymbol{G}_2^{(k)} = \boldsymbol{G}_1^{(k)}$, $\boldsymbol{B}_2^{(k)} = \bar{\gamma}_e\boldsymbol{Q}_k\hat{\boldsymbol{g}}_k^\dagger$, and $\boldsymbol{A}_2^{(k)} = \bar{\gamma}_e\boldsymbol{Q}_k$, $k = 1,\ldots,K$.

Proof: See Appendix E.

Last, we rewrite (44c) to facilitate the robust optimization against the errors introduced by $\Delta\boldsymbol{h}_k$'s. By applying Lemma 4.1, (44c) holds if and only if there exists $\mu_k \geq 0$, $k = 1,\ldots,K$, such that the following LMI constraint is met:

$$\begin{bmatrix} \eta P_s\boldsymbol{I} + \mu_k\boldsymbol{I} & \eta P_s\hat{\boldsymbol{h}}_k \\ \eta P_s\hat{\boldsymbol{h}}_k^H & \eta P_s\|\hat{\boldsymbol{h}}_k\|_2^2 - \mathrm{tr}(\boldsymbol{Q}_k) - \mu_k\epsilon_k' \end{bmatrix} \succeq \boldsymbol{0}, \forall k. \tag{67}$$

As such, $(\mathrm{P2}'.1\text{-RW-SDR-Eqv})$ is now simplified as

$$(\mathrm{P2}'.1\text{-}RW\text{-}SDR\text{-}Eqv): \max_{\boldsymbol{X},\{\boldsymbol{Q}_k\},\delta} \delta \quad \mathrm{s.t.} \quad (59),(63),(67),(44\mathrm{b}),(44\mathrm{e}).$$

Because of the non-convex term such as $\delta\boldsymbol{X}'$ in (59), problem $(\mathrm{P2}'.1\text{-RW-SDR-Eqv})$ remains very hard to solve. We thus use the bisection method [35] w.r.t. δ to solve it. However, using bisection in addition to solving $(\mathrm{P2}'.2)$ by one-dimension search over $\bar{\gamma}_e$ may lead to very high complexity. As a result, we propose an alternative problem to approximate $\hat{H}(\bar{\gamma}_e)$.

2) Solutions to $(\mathrm{P2}'.1\text{-RW-SDR})$*:* We propose to approximate $\hat{H}(\bar{\gamma}_e)$ by the optimum value of the following problem.

$$(\mathrm{P2}'.1\text{-RW-SDR}): \max_{\boldsymbol{X},\{\boldsymbol{Q}_k\},\tau} \min_{\tilde{\boldsymbol{h}}_0\in\tilde{\mathcal{H}}_0} P_s\mathrm{tr}(\boldsymbol{F}_1\boldsymbol{X}) \tag{68a}$$

$$\mathrm{s.t.} \max_{\substack{\tilde{\boldsymbol{h}}_k\in\tilde{\mathcal{H}}_k,\forall k\\ \tilde{\boldsymbol{h}}_0\in\tilde{\mathcal{H}}_0}} \sigma_r^2\mathrm{tr}(\overline{\boldsymbol{Y}}_1\boldsymbol{X}) + \sum_{k=1}^{K}\tilde{\boldsymbol{h}}_k^T\boldsymbol{Q}_k\tilde{\boldsymbol{h}}_k^\dagger + \tau\sigma_b^2 \leq 1, \tag{68b}$$

$$\max_{\substack{\boldsymbol{g}_k\in\mathcal{G}_k,\forall k\\ \boldsymbol{g}_0\in\mathcal{G}_0}} \frac{P_s\mathrm{tr}(\boldsymbol{F}_2\boldsymbol{X})}{\sigma_r^2\mathrm{tr}(\overline{\boldsymbol{Y}}_2\boldsymbol{X}) + \sum_{k=1}^{K}\boldsymbol{g}_k^T\boldsymbol{Q}_k\boldsymbol{g}_k^\dagger + \tau\sigma_e^2} \leq \bar{\gamma}_e, \tag{68c}$$

$$\mathrm{tr}(\overline{\boldsymbol{\Phi}}\boldsymbol{X}) \leq \tau P_r, \tag{68d}$$

$$\mathrm{tr}(\boldsymbol{Q}_k) \leq \tau\eta P_s \min_{\boldsymbol{h}_k\in\mathcal{H}_k,\forall k} \|\boldsymbol{h}_k\|^2, \forall k, \tag{68e}$$

$$\boldsymbol{X} \succeq \boldsymbol{0}, \boldsymbol{Q}_k \succeq \boldsymbol{0}, \forall k, \tau \geq 0. \tag{68f}$$

Remark 4.1: It is worth noting that as the numerator and the denominator of the objective function in $(\mathrm{P2}'.1)$ are coupled by common uncertainty $\tilde{\boldsymbol{h}}_0$, Charnes-Cooper transformation, in general, cannot be applied to realize equivalent decoupling. As a result, $(\mathrm{P2}'.1\text{-RW-SDR})$ yields a more conservative approximation for $\hat{H}(\bar{\gamma}_e)$ than $(\mathrm{P2}'.1\text{-RW-SDR-Eqv})$. However, considering that $(\mathrm{P2}'.1\text{-RW-SDR})$ needs to be solved only once for given $\bar{\gamma}_e$ in contrast with $(\mathrm{P2}'.1\text{-RW-SDR-Eqv})$ requring isection over δ, we exploit it in the sequel. The effectiveness of this approximation will be evaluated in Section V-B.

To proceed, we rewrite $(\mathrm{P2}'.1\text{-RW-SDR})$ as

$$(\mathrm{P2}'.1\text{-RW-SDR}): \max_{\boldsymbol{X},\{\boldsymbol{Q}_k\},\delta,\tau} \delta$$

$$\mathrm{s.t.} \min_{\tilde{\boldsymbol{h}}_0\in\tilde{\mathcal{H}}_0} P_s\mathrm{tr}(\boldsymbol{F}_1\boldsymbol{X}) \geq \delta, \tag{69a}$$

$$(68\mathrm{a})\text{-}(68\mathrm{f}). \tag{69b}$$

First, by rewriting $\boldsymbol{F} = \boldsymbol{f}_1^\dagger\boldsymbol{f}_1^T$, where $\boldsymbol{f}_1 = \hat{\boldsymbol{f}}_1 + \Delta\boldsymbol{f}_1$, in line with Lemma 4.1, the implication $\|\Delta\boldsymbol{f}_1\|^2 \leq \|\boldsymbol{h}_0\|^2\epsilon_0' \Rightarrow$ (69a) holds if and only if there exists $s'^{(0)} \geq 0$ such that the following LMI constraint is satisfied:

$$\begin{bmatrix} P_s\boldsymbol{X} + s'^{(0)}\boldsymbol{I} & P_s\boldsymbol{X}\hat{\boldsymbol{f}}_1^\dagger \\ P_s\hat{\boldsymbol{f}}_1^T\boldsymbol{X} & P_s\hat{\boldsymbol{f}}_1^T\boldsymbol{X}\hat{\boldsymbol{f}}_1^\dagger - s'^{(0)}\epsilon_0'\|\boldsymbol{h}_0\|_2^2 - \delta \end{bmatrix} \succeq \boldsymbol{0}. \tag{70}$$

Next, as $\mathrm{tr}(\overline{\boldsymbol{Y}}_1\boldsymbol{X}) = \boldsymbol{y}_1^T\boldsymbol{X}'\boldsymbol{y}_1^\dagger$ (cf. Equation (56)), where $\boldsymbol{y}_1 = \mathrm{vec}(\tilde{\boldsymbol{h}}_0^T \otimes \boldsymbol{I})$, after some manipulation, (68b) holds if and only if there exists $s''^{(0)} \geq 0$ such that

$$\begin{bmatrix} s''^{(0)}\boldsymbol{I} - \sigma_r^2\boldsymbol{X}' & -\sigma_r^2\boldsymbol{X}'\hat{\boldsymbol{y}}_1^\dagger \\ -\sigma_r^2\hat{\boldsymbol{y}}_1^T\boldsymbol{X}' & c \end{bmatrix} \succeq \boldsymbol{0}, \tag{71}$$

where $c = -\sigma_r^2\hat{\boldsymbol{y}}_1^T\boldsymbol{X}'\hat{\boldsymbol{y}}_1^\dagger - \sum_{k=1}^{K}\tilde{\boldsymbol{h}}_k^T\boldsymbol{Q}_k\tilde{\boldsymbol{h}}_k^\dagger - \tau\sigma_b^2 + 1 - s''^{(0)}N_t\epsilon_0'$. Then (68b) can be rewritten as

$$(71) \text{ for } \tilde{\boldsymbol{h}}_k \in \tilde{\mathcal{H}}_k, \forall k, \tag{72}$$

which is handled by the following proposition.

Proposition 4.3: The semi-indefinite constraints in (72) can be replaced by the following LMI constraint:

$$\begin{bmatrix} \bar{\boldsymbol{H}}^{(K)} & \bar{\boldsymbol{F}}^{(K)} & \bar{\boldsymbol{G}}^{(K)} \\ \bar{\boldsymbol{F}}^{(K)H} & \bar{c}^{(K)} & \bar{\boldsymbol{B}}^{(K)H} \\ \bar{\boldsymbol{G}}^{(K)H} & \bar{\boldsymbol{B}}^{(K)} & \bar{\boldsymbol{A}}^{(K)} \end{bmatrix} - s''^{(K)} \begin{bmatrix} \boldsymbol{0} & \boldsymbol{0} & \boldsymbol{0} \\ \boldsymbol{0} & 1 & \boldsymbol{0} \\ \boldsymbol{0} & \boldsymbol{0} & \frac{-\boldsymbol{I}}{\epsilon''_K} \end{bmatrix} \succeq \boldsymbol{0}, \tag{73}$$

where $\bar{\boldsymbol{H}}^{(K)}$ and $\bar{\boldsymbol{F}}^{(K)}$ are recursively given by

$$\begin{cases} \bar{\boldsymbol{H}}^{(k)} = \begin{bmatrix} \bar{\boldsymbol{A}}^{(k-1)} + \frac{s''^{(k-1)}\boldsymbol{I}}{\epsilon''_{k-1}} & \bar{\boldsymbol{G}}^{(k-1)H} \\ \bar{\boldsymbol{G}}^{(k-1)} & \bar{\boldsymbol{H}}^{(k-1)} \end{bmatrix}, \bar{\boldsymbol{F}}^{(k)} = \begin{bmatrix} \bar{\boldsymbol{B}}^{(k-1)} \\ \bar{\boldsymbol{F}}^{(k-1)} \end{bmatrix} \\ k = 2, \ldots, K; \\ \bar{\boldsymbol{H}}^{(1)} = s''^{(0)}\boldsymbol{I} - \sigma_r^2 \boldsymbol{X}', \bar{\boldsymbol{F}}^{(1)} = -\sigma_r^2 \boldsymbol{X}' \hat{\boldsymbol{y}}_1^\dagger, \end{cases} \tag{74}$$

where $\bar{\boldsymbol{G}}^{(k)} = \boldsymbol{G}_1^{(k)}$, $\bar{\boldsymbol{B}}^{(k)} = -\boldsymbol{Q}_k \hat{\tilde{\boldsymbol{h}}}_k^\dagger$, $\bar{\boldsymbol{A}}^{(k)} = -\boldsymbol{Q}_k$, $\bar{c}^{(k)} = -\sigma_r^2 \hat{\boldsymbol{y}}_1^T \boldsymbol{X}' \hat{\boldsymbol{y}}_1^\dagger - \Sigma_{j=1}^k \hat{\tilde{\boldsymbol{h}}}_j^T \boldsymbol{Q}_j \hat{\tilde{\boldsymbol{h}}}_j^\dagger - \Sigma_{i=k+1}^K \tilde{\boldsymbol{h}}_i^T \boldsymbol{Q}_i \tilde{\boldsymbol{h}}_i^\dagger - \tau\sigma_b^2 + 1 - s''^{(0)} N_t \epsilon'_0 - \Sigma_{l=1}^{k-1} s''^{(l)}$, $k = 1, \ldots, K$, and $\{s''^{(k)} \geq 0\}$ denote the auxiliary variables.

Proof: See Appendix F. ■

Proposition 4.4: The constraint in (68c) is guaranteed if and only if there exists $s^{(k)} \geq 0$, $k = 1, \ldots, K$, such that the following LMI holds:

$$\begin{bmatrix} \boldsymbol{H}^{(K)} & \boldsymbol{F}^{(K)} & \boldsymbol{G}^{(K)} \\ \boldsymbol{F}^{(K)H} & c'^{(K)} & \boldsymbol{B}'^{(K)H} \\ \boldsymbol{G}^{(K)H} & \boldsymbol{B}'^{(K)} & \boldsymbol{A}'^{(K)} \end{bmatrix} - s^{(K)} \begin{bmatrix} \boldsymbol{0} & \boldsymbol{0} & \boldsymbol{0} \\ \boldsymbol{0} & 1 & \boldsymbol{0} \\ \boldsymbol{0} & \boldsymbol{0} & \frac{-\boldsymbol{I}}{\epsilon_K} \end{bmatrix} \succeq \boldsymbol{0}, \tag{75}$$

where $\boldsymbol{H}^{(k)}$ and $\boldsymbol{F}^{(k)}$ are recursively given by

$$\begin{cases} \boldsymbol{H}^{(k)} = \begin{bmatrix} \boldsymbol{A}'^{(k-1)} + \frac{s^{(k-1)}\boldsymbol{I}}{\epsilon_{k-1}} & \boldsymbol{G}^{(k-1)H} \\ \boldsymbol{G}^{(k-1)} & \boldsymbol{H}^{(k-1)} \end{bmatrix}, \boldsymbol{F}^{(k)} = \begin{bmatrix} \boldsymbol{B}'^{(k-1)} \\ \boldsymbol{F}^{(k-1)} \end{bmatrix} \\ k = 2, \ldots, K; \\ \boldsymbol{H}^{(1)} = -P_s \boldsymbol{X}'' + \bar{\gamma}_e \sigma_r^2 \boldsymbol{X}' + s^{(0)}\boldsymbol{I}, \\ \boldsymbol{F}^{(1)} = (-P_s \boldsymbol{X}'' + \bar{\gamma}_e \sigma_r^2 \boldsymbol{X}')\hat{\boldsymbol{g}}^\dagger, \end{cases} \tag{76}$$

in which $\boldsymbol{G}^{(k)} = \boldsymbol{G}_1^{(k)}$, $\boldsymbol{B}'^{(k)} = \bar{\gamma}_e \boldsymbol{Q}_k \hat{\boldsymbol{g}}_k^\dagger$, $\boldsymbol{A}'^{(k)} = \bar{\gamma}_e \boldsymbol{Q}_k$, $c'^{(k)} = \hat{\boldsymbol{g}}^T(-P_s \boldsymbol{X}'' + \bar{\gamma}_e \sigma_r^2 \boldsymbol{X}')\hat{\boldsymbol{g}}^\dagger + \bar{\gamma}_e \sum_{j=1}^k \hat{\boldsymbol{g}}_j^T \boldsymbol{Q}_j \hat{\boldsymbol{g}}_j^\dagger + \bar{\gamma}_e \sum_{i=k+1}^K \boldsymbol{g}_i^T \boldsymbol{Q}_i \boldsymbol{g}_i^\dagger + \bar{\gamma}_e \tau \sigma_e^2 - s^{(0)} N_t \epsilon_0 - \sum_{l=1}^{k-1} s^{(l)}$, $k = 1, \ldots, K$, and $\{s^{(k)} \geq 0\}$ denote the auxiliary variables.

Proof: It is observed that (68c) differs from (44a) in the only respect that σ_e^2 is replaced by $\tau\sigma_e^2$. Hence the proof for Proposition 4.2 can be directly applied herein by substituting $\tau\sigma_e^2$ for σ_e^2. ■

Last, by replacing "ηP_s" in (44c) with "$\tau\eta P_s$" in (68e), (68e) can be replaced by a similar LMI as (67), denoted by (68e′), in which the pertinent auxiliary variables are denoted by $\{\mu_k \geq 0\}$.

Consequently, the equivalent reformulation for problem (P2′.1-RW-SDR) can be summarized as

$$\begin{aligned} (\text{P2}'.1\text{-RW-SDR}): \quad & \max_{\substack{\boldsymbol{X}, \{\boldsymbol{Q}_k\}, \delta, \tau, \\ s^{(0)}, s'^{(0)}, s''^{(0)}, \\ \{s^{(k)}\}, \{s''^{(k)}\}, \{\mu_k\}}} \quad \delta \\ \text{s.t.} \quad & (70), (73), (75), (68\text{e}'), (68\text{d}), (68\text{f}), \\ & s^{(0)} \geq 0, s'^{(0)} \geq 0, s''^{(0)} \geq 0, \qquad (77\text{a}) \\ & s^{(k)} \geq 0, s''^{(k)} \geq 0, \mu_k \geq 0, \forall k. \qquad (77\text{b}) \end{aligned}$$

C. Proposed Rank-One Solutions to (P2′.1)

(P2′.1-RW-SDR) is convex and can be solved efficiently by convex optimization tools such as CVX. Next, we derive the Lagrangian of (P2′.1-RW-SDR). Note that in the following expression, we only consider the uncertainties regarding $\tilde{\boldsymbol{h}}_0$, $\boldsymbol{h}_k$'s, $\tilde{\boldsymbol{h}}_k$'s, $\boldsymbol{g}_0$ and $\boldsymbol{g}_k$'s when $K = 1$ for the purpose of simplicity and the results can be easily extended to the case of $K > 1$. Denote the dual variables associated with (68d), (70), (73) and (75) by β_0, $\boldsymbol{W}$, $\boldsymbol{V}$ and $\boldsymbol{Y}$, respectively. Then the partial Lagrangian of (P2′.1-RW-SDR) w.r.t. $\boldsymbol{X}$ is

$$L(\overline{\boldsymbol{\Omega}}) = \text{tr}(\bar{\boldsymbol{A}}\boldsymbol{X}), \tag{78}$$

where $\overline{\boldsymbol{\Omega}}$ is the set of all primal and dual variables, and

$$\begin{aligned} \overline{\boldsymbol{A}} = & P_s \boldsymbol{W}_{1,1} + 2P_s \Re\{\hat{\boldsymbol{f}}_1^\dagger \boldsymbol{W}_{12}^T\} + P_s w_{2,2} \hat{\boldsymbol{F}}_1 \\ & - \sigma_r^2 \sum_{i=1}^{N_t} \left(\boldsymbol{V}_{1,1}^{(i,i)} + 2\Re\{\overline{\boldsymbol{V}}_{1,2}^{(i,i)}\} + \overline{\boldsymbol{V}}_{2,2}^{(i,i)} \right) \\ & - P_s(\boldsymbol{h}_0^H \otimes \boldsymbol{I})\boldsymbol{Y}_{1,1}(\boldsymbol{h}_0 \otimes \boldsymbol{I}) + 2\sigma_r^2 \bar{\gamma}_e \sum_{i=1}^{N_t^2} \Re\{\overline{\boldsymbol{Y}}_{2,1}^{(i,i)}\} \\ & - 2P_s \Re\{(\boldsymbol{h}_0^H \otimes \boldsymbol{I})\overline{\boldsymbol{Y}}_{2,1}(\boldsymbol{h}_0 \otimes \boldsymbol{I})\} \\ & - P_s y_{2,2}(\boldsymbol{h}_0^H \otimes \boldsymbol{I})\hat{\boldsymbol{g}}^\dagger \hat{\boldsymbol{g}}^T(\boldsymbol{h}_0 \otimes \boldsymbol{I}) + \sigma_r^2 \bar{\gamma}_e \sum_{i=1}^{N_t^2} \overline{\boldsymbol{Y}}_{2,2}^{(i,i)}. \end{aligned} \tag{79}$$

In (79), $\hat{\boldsymbol{F}}_1 = \hat{\boldsymbol{f}}_1^\dagger \hat{\boldsymbol{f}}_1^T$; $\boldsymbol{W}_{i,j}$, $i, j = 1, 2$, $\boldsymbol{V}_{i,j}$, $i, j = 1, \ldots, 3$ and $\boldsymbol{Y}_{i,j}$, $i, j = 1, \ldots, 3$ are the block submatrices of $\boldsymbol{W} \in \mathbb{C}^{(N_t^2+1)\times(N_t^2+1)}$, $\boldsymbol{V} \in \mathbb{C}^{(N_t^3+N_t+1)\times(N_t^3+N_t+1)}$ and $\boldsymbol{Y} \in \mathbb{C}^{(N_t^3+2N_t+1)\times(N_t^3+2N_t+1)}$ with the same size as block submatrices in (70), (73) and (75), respectively. Moreover, in (79), $\overline{\boldsymbol{V}}_{1,2} = \hat{\boldsymbol{y}}_1^\dagger \boldsymbol{V}_{1,2}^T$, $\overline{\boldsymbol{V}}_{2,2} = v_{2,2}\hat{\boldsymbol{y}}_1^\dagger \hat{\boldsymbol{y}}_1^T$, $\overline{\boldsymbol{Y}}_{2,1} = \hat{\boldsymbol{g}}^\dagger \boldsymbol{y}_{1,2}^T$ and $\overline{\boldsymbol{Y}}_{2,2} = y_{2,2}\hat{\boldsymbol{g}}^\dagger \hat{\boldsymbol{g}}^T$. Furthermore, $\boldsymbol{V}_{1,1}^{(i,i)}$, $\overline{\boldsymbol{V}}_{1,2}^{(i,i)}$ and $\overline{\boldsymbol{V}}_{2,2}^{(i,i)}$ are the ith block diagonal submatrices of $\boldsymbol{V}_{1,1} \in \mathbb{C}^{N_t^3 \times N_t^3}$, $\overline{\boldsymbol{V}}_{1,2} \in \mathbb{C}^{N_t^3 \times N_t^3}$ and $\overline{\boldsymbol{V}}_{2,2} \in \mathbb{C}^{N_t^3 \times N_t^3}$, respectively; $\overline{\boldsymbol{Y}}_{2,1}^{(i,i)}$ and $\overline{\boldsymbol{Y}}_{2,2}^{(i,i)}$ are the ith block diagonal submatrices of $\boldsymbol{Y}_{2,1} \in \mathbb{C}^{N_t^3 \times N_t^3}$, and $\overline{\boldsymbol{Y}}_{2,2} \in \mathbb{C}^{N_t^3 \times N_t^3}$, respectively.

Proposition 4.5:

1) The optimal $\boldsymbol{X}^*$ to (P2′.1-RW-SDR) is expressed as

$$\boldsymbol{X}^* = \sum_{n=1}^{N_t^2 - \bar{r}_c} \bar{a}_n \bar{\boldsymbol{\eta}}_n \bar{\boldsymbol{\eta}}_n^H + \bar{b}\bar{\boldsymbol{\xi}}\bar{\boldsymbol{\xi}}^H, \tag{80}$$

where $\bar{a}_n \geq 0, \forall n$, $\bar{b} > 0$, and $\bar{\boldsymbol{\xi}} \in \mathbb{C}^{N_t^2 \times 1}$ is a unit-norm vector orthogonal to $\bar{\boldsymbol{\Xi}}$ (cf. Equation (28)).

2) According to (80), if $\text{rank}(\boldsymbol{X}^*) > 1$, i.e., there exists at least one $\bar{a}_n > 0$, we reconstruct a solution to problem (P2′.1-RW-SDR) using

$$\hat{\boldsymbol{X}}^* = \bar{b}\bar{\boldsymbol{\xi}}\bar{\boldsymbol{\xi}}^H, \tag{81}$$

$$\hat{\delta}^* = \delta^*, \tag{82}$$

$$\hat{\tau}^* = \tau^*, \tag{83}$$

TABLE II
ALGORITHM II FOR (P2′)

- **Initialize** $\bar{\gamma}'_{e_\text{search}} = 0 : \alpha' : \bar{\gamma}'_{e\,\max}$ and $i = 0$
- **Repeat**
  1) **Set** $i = i + 1$;
  2) Given $\bar{\gamma}_e = \bar{\gamma}'_{e_\text{search}}(i)$,
     solve (P2′.1-RW-SDR) and **obtain** $\hat{H}(\bar{\gamma}_e^{(i)})$.
- **Until** $i = L'$, where $L' = \lfloor \frac{\bar{\gamma}'_{e\,\max}}{\alpha'} \rfloor + 1$ is the length of $\bar{\gamma}'_{e_\text{search}}$
- **Set** $\bar{\gamma}_e^* = \bar{\gamma}'_{e_\text{search}} \left(\arg\max_i \left\{ \frac{1+\hat{H}(\bar{\gamma}_e^{(i)})}{1+\bar{\gamma}_e^{(i)}} \right\} \right)$ for (P2′.2)
- Given $\bar{\gamma}_e^*$, **solve** (P2′.1-RW-SDR) to obtain $(\boldsymbol{X}^*, \{\boldsymbol{Q}_k^*\}, \delta^*, \tau^*)$
  if $\text{rank}(\boldsymbol{X}^*) = 1$, **apply** EVD on $\boldsymbol{X}^*$ such that $\boldsymbol{X}^* = \boldsymbol{w}^* \boldsymbol{w}^{*H}$;
  else
  – **construct** $(\hat{\boldsymbol{X}}^*, \hat{\delta}^*, \hat{\tau}^*)$, according to (81)-(83) and **set** $\boldsymbol{w}^* = \sqrt{\bar{b}}\boldsymbol{\xi}$;
  – given $\hat{\boldsymbol{X}}^*$, $\hat{\delta}^*$ and $\hat{\tau}^*$,
  obtain $\{\hat{\boldsymbol{Q}}_k^*\}$ by solving (P2′.1-RW-SDR-sub).
  end
- **Recover** $\boldsymbol{W}^* = \text{vec}^{-1}(\boldsymbol{w}^*)$

while $\{\hat{\boldsymbol{Q}}_k^*\}$ are obtained by solving the following feasibility problem provided that $\hat{\boldsymbol{X}}^*$, $\hat{\delta}^*$, and $\hat{\tau}^*$ are given by (81), (82) and (83), respectively:

$$\begin{aligned}
&(\text{P2}'.1\text{-RW-SDR-sub}): \max_{\substack{\{\boldsymbol{Q}_k\}, s''^{(0)}, \\ \{s''^{(k)}\}, \{\mu_k\}}} \quad 0 \\
&\text{s.t.} \ (73) \text{ given } \hat{\boldsymbol{X}}^*, \hat{\tau}^*, (68\text{e}') \text{ given } \hat{\tau}^*, \\
&\boldsymbol{Q}_k \succeq \boldsymbol{0}, \mu_k \geq 0, \forall k, \\
&s''^{(0)} \geq 0, s''^{(k)} \geq 0, \forall k.
\end{aligned}$$

Proof: See Appendix G. ■

The scheme that solves (P2′) is summarized in Table II.

V. NUMERICAL RESULTS

Here we provide numerical examples to validate our results. We assume a typical scenario where the K helpers are evenly distributed around Alice with a radius of $\rho_k = 2$ m and $\theta_k = \frac{2\pi(k-1)}{K}$ (radian by default), where θ_k is the angle of direction (w.r.t. the Alice-relay link by default) of the kth helper, $k = 1, \ldots, K$. Alice, Bob and Eve are, w.l.o.g., assumed to have the same distance away from the AF relay with their angle of direction π, $\pi/6$ and $11\pi/6$, respectively. We also assume channel models with both large-scale fading, i.e., path loss and shadowing, and small-scale fading, i.e., multi-path fading. The simplified large-scale fading model is given by [39]

$$D = zA_0 \left(\frac{d}{d_0} \right)^{-\alpha}, \text{ for } d \geq d_0, \tag{84}$$

where z is a log-normal random variable capturing the effect of shadowing with the standard derivation $\sigma = 4$ dB, $A_0 = 10^{-3}$, d is the distance, d_0 is a reference distance set to be 1 m, and $\alpha = 2$ is the path loss exponent. Specifically, the channels including $\boldsymbol{h}_k$'s, $\boldsymbol{h}_0$, $\tilde{\boldsymbol{h}}_0$ and $\boldsymbol{g}_0$, are assumed to suffer from Rician fading while the channels from the HJ helpers to Bob ($\tilde{\boldsymbol{h}}_k$'s) and Eve ($\boldsymbol{g}_k$'s) follow Rayleigh distribution due to the missing of line-of-sight (LOS) components with their respective average gain specified by (84). Take $\boldsymbol{h}_k, \forall k$, as an example, $\boldsymbol{h}_k = \sqrt{\frac{K_R}{K_R+1}}\bar{\boldsymbol{h}}_k + \sqrt{\frac{1}{K_R+1}}\check{\boldsymbol{h}}_k$, where $\bar{\boldsymbol{h}}_k$ is the LOS component with $\|\bar{\boldsymbol{h}}_k\|_2^2 = D$ (cf. Equation (84)), $\check{\boldsymbol{h}}_k$ is the Rayleigh fading component denoted by $\check{\boldsymbol{h}}_k \sim \mathcal{CN}(0, D\boldsymbol{I})$, and K_R is the Rician factor set to be 3. Note that for the involved LOS component, we use the far-field uniform linear antenna array to model the channels [40]. In addition, unless otherwise specified, the number of HJ helpers, K is set to be 5; the AF relay is assumed to be 5 m away from Alice; the EH efficiency, $\eta = 0.5$ and $\sigma_r^2 = \sigma_b^2 = \sigma_e^2 = -50$ dBm. The results presented in Section V-A are obtained by averaging over 500 times of independent trials.

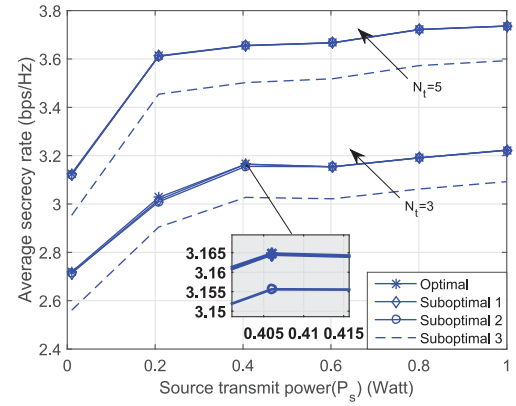

Fig. 2. Secrecy rate versus Alice's transmit power with perfect CSI.

A. The Perfect CSI Case

We compare the proposed optimal solutions with three suboptimal schemes in the case of perfect CSI. One suboptimal scheme, denoted by "Suboptimal 1", is introduced in Section III-C1 by exploiting the optimal structure of $\boldsymbol{W}$. The other described in Section III-C2 is known as optimal null-space ZF, denoted by "Suboptimal 2". Specifically, each jamming beam $\boldsymbol{n}_k$ is restricted to lie in the orthogonal space of $\tilde{\boldsymbol{h}}_k^\dagger$ such that $\boldsymbol{n}_k$'s cause no interference to the IR while maximizing its effect of jamming at the eavesdropper. As a benchmark, we also present the well-known *isotropic jamming* that is particularly useful when there is no Eve's CSI known at each *HJ* helper, $\mathsf{H}_k, \forall k$ [41], denoted by "Suboptimal 3". Note that the difference between "Suboptimal 2" and "Suboptimal 3" only lies in the design of jamming noise, for which the former also aligns the jamming noise to an equivalent Eve's channel to confront Eve with most interference, while the latter transmits isotropic jamming with $\tilde{\boldsymbol{n}}_k \sim \mathcal{CN}(\boldsymbol{0}, \eta P_s \|\boldsymbol{h}_k\|^2/(N_t - 1))$, $k = 1, \ldots, K$, in directions orthogonal to $\tilde{\boldsymbol{h}}_k$'s, due to lack of knowledge of Eve's channel and thus is expected to be less efficient than "Suboptimal 2" with perfect CSI.

First, we study the secrecy rate at the receiver versus the transmit power of the transmitter, P_s with $P_r = 10$ dBm. Fig. 2 demonstrates that for both cases of $N_t = 3$ and $N_t = 5$, the average secrecy rate increases and tends to be saturated as P_s goes to 30 dBm. It also illustrates that "suboptimal 1" and "suboptimal 2" closely approach the optimal solutions while "Suboptimal 3" is outperformed more succinctly with larger number of antennas at the AF relay and the HJ helpers. Moreover, with N_t increasing, the average secrecy rate gets larger as a result of the higher array gain of the AF relay and more available power transferred to the HJ helpers.

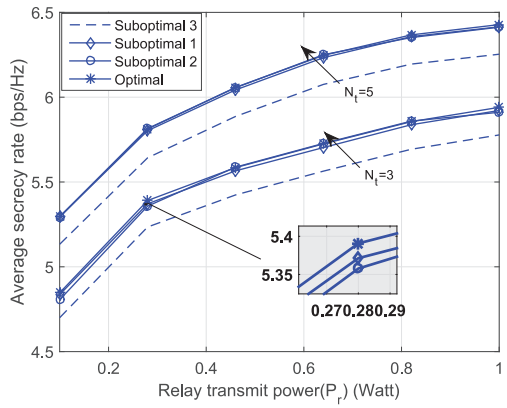

Fig. 3. Secrecy rate versus the relay's transmit power with perfect CSI.

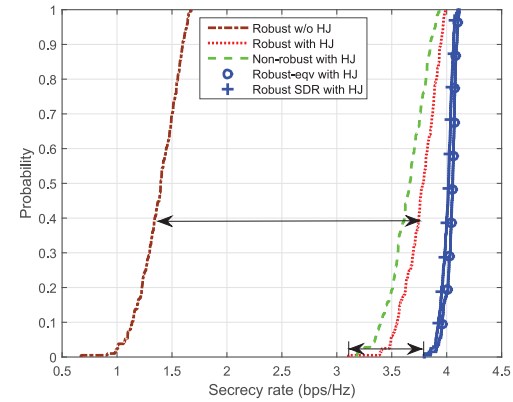

Fig. 4. CDFs of the achievable secrecy rate.

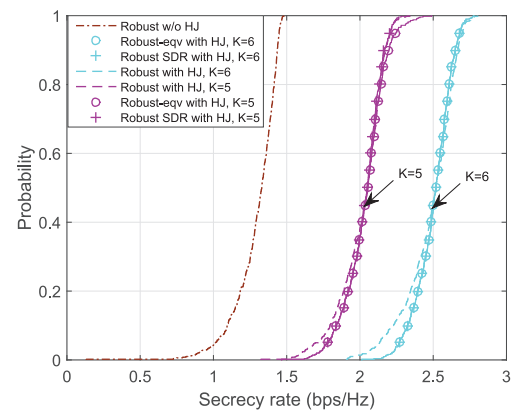

Fig. 5. Secrecy outage probability for $K = 3$ and $K = 5$ HJ helpers, respectively.

In addition, we show in Fig. 3 the secrecy rate achieved by different schemes versus the transmit power of the AF relay, P_r with $P_s = 30$ dBm. It is seen that the average secrecy rate first grows faster and then slower, since when P_r increases, not only the desired signal but also the noise yielded from the first transmission phase is amplified to a larger extent. In addition, the performance gap between the optimal scheme and suboptimal schemes is almost negligible. Similar to Fig. 2, "Suboptimal 3" appears to have certain performance loss from the optimality but is considered as a promising scheme when no Eve's CSI is available at the HJ helpers.

B. The Imperfect CSI Case

Now, we consider the imperfect CSI case and compare the proposed scheme *Robust SDR with HJ*, which is obtained by solving $(\mathrm{P2'.1\text{-}RW\text{-}SDR\text{-}sub})$, against some benchmarks. Note that there are two upper-bound benchmark schemes, namely, *Robust SDR with HJ* and *Robust-eqv with HJ*, as well as two lower-bound benchmarks, which are *Robust w/o HJ* and *Non-robust with HJ*. For *Robust SDR with HJ* (*Robust-eqv with HJ*), given any $\bar{\gamma}_e$, $\hat{H}(\bar{\gamma}_e)$ is approximated by solving the rank constraint relaxed problem $(\mathrm{P2'.1\text{-}RW\text{-}SDR})((\mathrm{P2'.1\text{-}RW\text{-}SDR\text{-}Eqv}))$. On the other hand, for *Robust w/o HJ*, we solve $(\mathrm{P2'.1\text{-}RW\text{-}SDR})$ by setting $\boldsymbol{Q}_k = 0, \forall k$ while for *Non-robust with HJ*, (11) is evaluated by applying the optimal solutions to $(\mathrm{P1'.1})$ assuming perfect CSI, to the actual channels including errors that are generated from the sets defined in (41).

To assess the worst-case secrecy performance, we use the metric, namely, *secrecy outage probability*, defined as [42]:

$$p = P_r(r \leq r_0^*), \tag{85}$$

where r_0^* obtained by solving $(\mathrm{P2'})$ is termed as the $100p\%$-*secrecy outage rate*.

The parameters are set identical to those in the perfect CSI case. Regarding the uncertainty model in (41), we introduce the uncertainty ratios associated with ϵ_0, ϵ_0', ϵ_k, ϵ_k' and ϵ_k'' as α_0, α_0', α_k, α_k' and α_k'', respectively. For instance, α_0 is

$$\alpha_0^2 = \frac{\epsilon_0}{\mathbb{E}[\|\boldsymbol{g}_0\|^2]}, \tag{86}$$

while α_0', α_k's, α_k''s and α_k'''s are similarly defined and thus omitted here for brevity. Besides, it is reasonable to assume that the channel estimates w.r.t Eve suffer from more errors than those for Alice and Bob. Hence, we set $\alpha_0'^2 = \alpha_k'^2 = \alpha_k''^2 = 1\%$ while $\alpha_0^2 = \alpha_k^2 = 10\%$, $k = 1, \ldots, K$, unless otherwise specified.

Fig. 4 demonstrates the cumulative density function (CDF) of the achievable secrecy rate from 1000 samples of random channel errors uniformly distributed over the sets defined by (41) given fixed actual channel realization. We set $P_r = 20$ dBm, $P_s = 30$ dBm, $N_t = 3$, $K = 5$ and $\alpha_0'^2 = \alpha_k'^2 = \alpha_k''^2 = 2\%$, $k = 1, \ldots, K$. Despite being suboptimal to the upper-bound schemes of "Robust SDR with HJ" and "Robust-eqv with HJ", the proposed "Robust with HJ" scheme outperforms its non-robust counterpart "Non-robust with HJ" particularly in the low range of probability, and overwhelmingly surpasses the "Robust w/o HJ". For example, "Robust with HJ" can achieve a secrecy rate of around 3.5 bps/Hz in the 3% worst case versus that of 3.3 bps/Hz and 1.0 bps/Hz for the "Non-robust with HJ" and "Robust w/o HJ", respectively. The solutions for "Robust SDR with HJ" is also seen to admit very little gap from those for "Robust-eqv with HJ", which suggests that approximating $\hat{H}(\bar{\gamma}_e)$ by solving the complexity reduced "Robust SDR with HJ" leads almost no performance loss.

Fig. 5 illustrates the CDF of the achievable secrecy rate from 1000 samples of random channel errors generated in the same way as Fig. 4, with $P_r = 20$ dBm, $P_s = 30$ dBm and $N_t = 3$. It is observed that proposed solutions to "Robust with HJ"

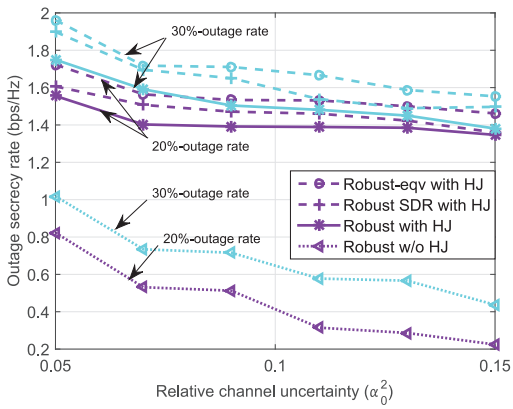

Fig. 6. Secrecy outage rate versus the normalized channel errors.

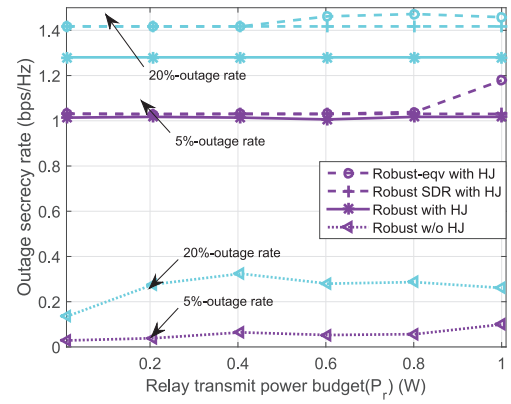

Fig. 7. Secrecy outage rate versus the relay's transmit power.

nearly achieve their upper-bound rank constraint relaxed solutions, i.e., SDR, to "Robust upper SDR with HJ" throughout the whole range of outage probability. Moreover, the "Robust w/o HJ" yields the worst performance. In particular, when the outage probability falls to 3%, the "Robust w/o HJ" achieves a worst-case secrecy rate of less than 1 bps/Hz while the proposed scheme can still guarantee an outage rate of rough 1.64 bps/Hz and 2.07 bps/Hz for $K = 5$ and $K = 6$, respectively. Also, it is observed that increasing the number of HJ helpers will improve the secrecy performance, but we do not draw conclusions on the extent to which the secrecy rate can increase, since it also depends on the level of channel estimation inaccuracy. For example, more HJ helpers may also yield larger interference to the legitimate receiver if the channels from HJ helpers to Bob are not as well estimated as this instance of $\alpha_k''^2 = 1\%, \forall k$. Hence we suggest that in practice, a mild number of HJ helpers are sufficient in view of the trade-off between complexity and performance.

Fig. 6 shows two different levels ($p = 0.20$ and $p = 0.30$) of secrecy outage rate versus the channel uncertainty ratios (assuming $\alpha_0 = \alpha_k$, $k = 1, \ldots, K$), in which $P_r = 30$ dBm, $P_s = 30$ dBm, $N_t = 3$ and $K = 5$. It is observed that the secrecy outage rate by the proposed schemes decreases slowly with the eavesdropper's CSI error ratios, which validates the motivation of the worst-case robust optimization. It is worth noting that the advantage of the *HJ* protocol is more significant when the normalized channel uncertainty of Eve's channels surpasses 10%, since the *HJ* scheme provides more degree of freedom for robust design and thus capable of guaranteeing larger worst-case secrecy rate against worse channel conditions compared to that without *HJ*. The reasonably suboptimal performance of the proposed "Robust with HJ" is also seen as from Figs. 4 and 5.

Fig. 7 studies the 100 p%-secrecy outage rate for $p = 0.05$ and $p = 0.20$, respectively, versus the transmit power of the AF relay. Specifically, we set $P_s = 30$ dBm, $N_t = 3$, and $K = 5$. As observed similarly from Fig. 6, the robust schemes with the assistance of HJ helpers perform considerably better than solutions without HJ helpers. Furthermore, when the transmit power is set relatively large, i.e., $P_s = 30$ dBm, it is seen that continuously increasing P_r does not contribute much to the secrecy performance, because in this situation the increased amplified noise at the AF relay compromises the performance, which provides useful insight for practical setting of P_r. In addition, the proposed "Robust with HJ" is observed striking a good trade-off between optimality and complexity compared with the two upper-bound solutions.

VI. Conclusion

This paper considered improving the secret wireless communications in a multi-antenna AF relay wiretap channel via a novel *harvest-and-jam (HJ)* relaying protocol. The AN covariance matrices at HJ helpers and the AF relay beamforming matrix have been jointly optimized to maximize the achievable secrecy rate and/or worst-case secrecy rate at the legitimate receiver subject to the transmit power constraints of the AF relay as well as the HJ helpers, on perfect and imperfect CSI occasions, respectively, using the technique of semi-definite relaxation (SDR). The SDR was shown tight for the perfect CSI case while suboptimal rank-one reconstruction algorithms for the robust formulation under imperfect CSIs were presented achieving promising tradeoffs between complexity and performance. The effectiveness of the proposed schemes were also verified by numerical results.

Appendix

A. Proof of Proposition 3.1

The KKT conditions of (P1′.1-RW-SDR) are given by

$$\boldsymbol{A}^*\boldsymbol{X}^* = 0, \tag{87a}$$

$$\boldsymbol{B}_k^*\boldsymbol{Q}_k^* = 0, \forall k, \tag{87b}$$

$$\beta_k^*\left(\mathrm{tr}(\boldsymbol{Q}_k^*) - \tau^*\eta P_s\|\boldsymbol{h}_k\|^2\right) = 0, \forall k. \tag{87c}$$

According to (26), if for certain k, $\beta_k^* = 0$, then $\boldsymbol{B}_k^* = -\lambda^*\tilde{\boldsymbol{h}}_k^*\tilde{\boldsymbol{h}}_k^T + \alpha^*\bar{\gamma}_e\boldsymbol{g}_k^*\boldsymbol{g}_k^T$ and thus $\mathrm{rank}(\boldsymbol{B}_k^*) \le \mathrm{rank}(\tilde{\boldsymbol{h}}_k^*\tilde{\boldsymbol{h}}_k^T) + \mathrm{rank}(\boldsymbol{g}_k^*\boldsymbol{g}_k^T) = 2$, which yields $\mathrm{rank}(\boldsymbol{Q}_k^*) \ge N_t - 2$ as a result of (87b). Otherwise, when $\beta_k^* > 0$, we will have $\mathrm{rank}(\boldsymbol{B}_k^*) \ge \mathrm{rank}(-\beta_k^*\boldsymbol{I} - \lambda^*\tilde{\boldsymbol{h}}_k^*\tilde{\boldsymbol{h}}_k^T) - \mathrm{rank}(\alpha^*\bar{\gamma}_e\boldsymbol{g}_k^*\boldsymbol{g}_k^T) = N_t - 1$ [7, Lemma A.1], which implies $\mathrm{rank}(\boldsymbol{Q}_k^*) \le 1$. However, $\mathrm{rank}(\boldsymbol{Q}_k^*)$ cannot be 0, since otherwise $\mathrm{tr}(\boldsymbol{Q}_k^*) - \tau^*\eta P_s\|\boldsymbol{h}_k\|^2 < 0$ and thus $\beta_k^* = 0$ according to (87c), which contradicts to $\beta_k^* > 0$. Hence, when $\beta_k^* > 0$, $\mathrm{rank}(\boldsymbol{Q}_k^*) = 1$.

Next, define $\boldsymbol{C}^* = -\lambda^*\sigma_r^2\overline{\boldsymbol{Y}}_1 - \alpha^*P_s\boldsymbol{F}_2 + \alpha^*\bar{\gamma}_e\sigma_r^2\overline{\boldsymbol{Y}}_2 - \beta_0^*\overline{\boldsymbol{\Phi}}$ and according to (25), we have

$$\boldsymbol{A}^* = P_s\boldsymbol{F}_1 + \boldsymbol{C}^*. \tag{88}$$

Then define r_c, Ξ and $\boldsymbol{\eta}_n$, $n = 1, \ldots, N_t^2 - r_c$ (cf. Equation (28)). Similar to the approach used in [7, Appendix B], we discuss the structure of the optimal $\boldsymbol{X}$ under two cases.

1) Case I: $r_c = N_t^2$. As $\boldsymbol{C}^*$ is full-rank, $\text{rank}(\boldsymbol{A}^*) \geq r_c - 1 = N_t^2 - 1$ and hence $N_t^2 - 1 \leq \text{rank}(\boldsymbol{A}^*) \leq N_t^2$. If $\text{rank}(\boldsymbol{A}^*) = N_t^2 - 1$, $\text{rank}(\textbf{null}(\boldsymbol{A}^*)) = 1$ and it follows that $\boldsymbol{X}^* = b\boldsymbol{\xi}\boldsymbol{\xi}^H$ by assuming $\boldsymbol{\xi}$ as the only basis of $\textbf{null}(\boldsymbol{A}^*)$. Otherwise, according to (87a), we obtain $\boldsymbol{X}^* = \boldsymbol{0}$, which ceases the secrecy transmission and cannot be the optimal solution to (P1′.1-RW-SDR).
2) Case II: $r_c < N_t^2$. If $\boldsymbol{C}^*$ is not full-rank, $\text{rank}(\boldsymbol{A}^*) \geq r_c - 1$. Then by pre-multiplying $\boldsymbol{\eta}_n^H$ and post-multiplying $\boldsymbol{\eta}_n \in \Xi$ with both sides of (88), we have

$$\boldsymbol{\eta}_n^H \boldsymbol{A}^* \boldsymbol{\eta}_n = P_s \boldsymbol{\eta}_n^H \boldsymbol{F}_1 \boldsymbol{\eta}_n + \boldsymbol{\eta}_n^H \boldsymbol{C}^* \boldsymbol{\eta}_n = P_s \boldsymbol{\eta}_n^H \boldsymbol{F}_1 \boldsymbol{\eta}_n, \forall n. \quad (89)$$

According to (24), it is necessary for $\boldsymbol{A}^* \preceq \boldsymbol{0}$ to obtain an optimal solution of $\boldsymbol{X}^*$ and therefore $\boldsymbol{\eta}_n^H \boldsymbol{A}^* \boldsymbol{\eta}_n \leq 0$, which conforms to $P_s \boldsymbol{\eta}_n^H \boldsymbol{F}_1 \boldsymbol{\eta}_n \geq 0$ if and only if $\boldsymbol{A}^* \boldsymbol{\eta}_n = 0$ and $\boldsymbol{F}_1 \boldsymbol{\eta}_n = 0$. Hence, $\Xi \subseteq \textbf{null}(\boldsymbol{A}^*)$, i.e., $N_t^2 - \text{rank}(\boldsymbol{A}^*) \geq N_t^2 - r_c \Rightarrow \text{rank}(\boldsymbol{A}^*) \leq r_c$. Next, we show $\text{rank}(\boldsymbol{A}^*) \neq r_c$ by contradiction. If $\text{rank}(\boldsymbol{A}^*) = r_c$, $\Xi = \textbf{null}(\boldsymbol{A}^*)$, and $\boldsymbol{X}^* = \sum_{n=1}^{N_t^2 - r_c} a_n \boldsymbol{\eta}_n \boldsymbol{\eta}_n^H$. However, in this case, since $\boldsymbol{F}_1 \boldsymbol{\eta}_n = 0$, $P_s \text{tr}(\boldsymbol{F}_1 \boldsymbol{X}^*) = 0$, which is apparently not optimal. Hence, we have $\text{rank}(\boldsymbol{A}^*) = r_c - 1$ and thus $\text{rank}(\textbf{null}(\boldsymbol{A}^*)) = N_t^2 - r_c + 1$. This indicates that besides the basis in Ξ, $\textbf{null}(\boldsymbol{A}^*)$ spans over an extra dimension of basis, which is denoted by $\boldsymbol{\xi}$, and hence $\boldsymbol{X}^* = \sum_{n=1}^{N_t^2 - r_c} a_n \boldsymbol{\eta}_n \boldsymbol{\eta}_n^H + b\boldsymbol{\xi}\boldsymbol{\xi}^H$.

Assume that $(\boldsymbol{X}^*, \{\boldsymbol{Q}_k^*\}, \tau^*)$ is the optimal solution to (P1′.1-RW-SDR) with $\text{rank}(\boldsymbol{X}^*) > 1$. Then construct a new solution $\{\hat{\boldsymbol{X}}^*, \hat{\boldsymbol{Q}}_k^*, \hat{\tau}^*\}$ according to (29)–(31). Now, we check if the reconstructed solution is feasible if (32) holds. First,

$$\begin{aligned}
&\sigma_r^2 \text{tr}(\overline{\boldsymbol{Y}}_1 \hat{\boldsymbol{X}}^*) + \sum_{k=1}^{K} \tilde{\boldsymbol{h}}_k^T \hat{\boldsymbol{Q}}_k^* \tilde{\boldsymbol{h}}_k^\dagger + \hat{\tau}^* \sigma_b^2 \\
&\leq \sigma_r^2 \text{tr}\left(\overline{\boldsymbol{Y}}_1 \left(\boldsymbol{X}^* - \sum_{n=1}^{N_t^2 - r_c} a_n \boldsymbol{\eta}_n \boldsymbol{\eta}_n^H\right)\right) + \sum_{k=1}^{K} \tilde{\boldsymbol{h}}_k^T \boldsymbol{Q}_k^* \tilde{\boldsymbol{h}}_k^\dagger \\
&\quad + \left(\tau^* + \frac{\sigma_r^2}{\sigma_b^2} \sum_{n=1}^{N_t^2 - r_c} a_n \text{tr}(\overline{\boldsymbol{Y}}_1 \boldsymbol{\eta}_n \boldsymbol{\eta}_n^H)\right) \sigma_b^2 \\
&= \sigma_r^2 \text{tr}(\overline{\boldsymbol{Y}}_1 \boldsymbol{X}^*) + \sum_{k=1}^{K} \tilde{\boldsymbol{h}}_k^T \boldsymbol{Q}_k^* \tilde{\boldsymbol{h}}_k^\dagger + \tau^* \sigma_b^2 \overset{(a)}{\leq} 1.
\end{aligned} \quad (90)$$

Moreover,

$$\begin{aligned}
&P_s \text{tr}(\boldsymbol{F}_2 \hat{\boldsymbol{X}}^*) = P_s \text{tr}\left(\boldsymbol{F}_2 (\boldsymbol{X}^* - \sum_{n=1}^{N_t^2 - r_c} a_n \boldsymbol{\eta}_n \boldsymbol{\eta}_n^H)\right) \\
&\overset{(b)}{\leq} \bar{\gamma}_e \left(\sigma_r^2 \text{tr}(\overline{\boldsymbol{Y}}_2 \boldsymbol{X}^*) + \sum_{k=1}^{K} \boldsymbol{g}_k^T \boldsymbol{Q}_k^* \boldsymbol{g}_k^\dagger + \tau^* \sigma_e^2\right) \\
&\quad + \bar{\gamma}_e \left(\sigma_e^2 \Delta\tau - \sigma_r^2 \text{tr}\left(\overline{\boldsymbol{Y}}_2 \sum_{n=1}^{N_t^2 - r_c} a_n \boldsymbol{\eta}_n \boldsymbol{\eta}_n^H\right)\right) \\
&= \bar{\gamma}_e \left(\sigma_r^2 \text{tr}(\overline{\boldsymbol{Y}}_2 \hat{\boldsymbol{X}}^*) + \sum_{k=1}^{K} \boldsymbol{g}_k^T \hat{\boldsymbol{Q}}_k^* \boldsymbol{g}_k^\dagger + \hat{\tau}^* \sigma_e^2\right).
\end{aligned} \quad (91)$$

In addition, (23c)–(23e) are easily shown to satisfy. In the above, (a) and (b) hold due to the feasibility in (23a) and (23b), respectively. Further, $P_s \text{tr}(\boldsymbol{F}_1 \hat{\boldsymbol{X}}^*) = P_s \text{tr}(\boldsymbol{F}_1 \boldsymbol{X}^*)$ shows that the reconstructed solution achieves the same optimum value as that of (P1′.1-RW-SDR). Hence, an optimal solution to (P1′.1-RW-SDR) with rank-one $\boldsymbol{X}$ is ensured.

B. Proof of Lemma 3.3

First, we construct $\boldsymbol{W}$ as

$$\begin{aligned}
\boldsymbol{W} &= [\boldsymbol{U}_1^\dagger, (\boldsymbol{U}_1^\perp)^\dagger] \begin{bmatrix} \boldsymbol{B} & \boldsymbol{C} \\ \boldsymbol{D} & \boldsymbol{E} \end{bmatrix} [\boldsymbol{U}_2, \boldsymbol{U}_2^\perp]^H \\
&= \boldsymbol{U}_1^\dagger \boldsymbol{B} \boldsymbol{U}_2^H + \boldsymbol{U}_1^\dagger \boldsymbol{C} (\boldsymbol{U}_2^\perp)^H + (\boldsymbol{U}_1^\perp)^\dagger \boldsymbol{D} \boldsymbol{U}_2^H \\
&\quad + (\boldsymbol{U}_1^\perp)^\dagger \boldsymbol{E} (\boldsymbol{U}_2^\perp)^H,
\end{aligned} \quad (92)$$

where $\boldsymbol{B} \in \mathbb{C}^{2\times 2}$, $\boldsymbol{C} \in \mathbb{C}^{2\times(N_t-2)}$, $\boldsymbol{D} \in \mathbb{C}^{(N_t-2)\times 2}$ and $\boldsymbol{E} \in \mathbb{C}^{(N_t-2)\times(N_t-2)}$ are undetermined matrices. Then according to (33) and (34), it follows that $|\tilde{\boldsymbol{h}}_0^T \boldsymbol{W} \boldsymbol{h}_0|^2 = |\tilde{\boldsymbol{h}}_0^T \boldsymbol{U}_1^\dagger \boldsymbol{B} \boldsymbol{U}_2^H \boldsymbol{h}_0|^2$ and $\tilde{\boldsymbol{h}}_0^T \boldsymbol{W} \boldsymbol{W}^H \tilde{\boldsymbol{h}}_0^\dagger = \|\boldsymbol{B}^H \boldsymbol{U}_1^T \tilde{\boldsymbol{h}}_0^\dagger\|^2 + \|\boldsymbol{C}^H \boldsymbol{U}_1^T \tilde{\boldsymbol{h}}_0^\dagger\|^2$. Similarly, we also have $|\boldsymbol{g}_0^T \boldsymbol{W} \boldsymbol{h}_0|^2 = |\boldsymbol{g}_0^T \boldsymbol{U}_1^\dagger \boldsymbol{B} \boldsymbol{U}_2^H \boldsymbol{h}_0|^2$ and $\boldsymbol{g}_0^T \boldsymbol{W} \boldsymbol{W}^H \boldsymbol{g}_0^\dagger = \|\boldsymbol{g}_0^T \boldsymbol{U}_1^\dagger \boldsymbol{B}\|^2 + \|\boldsymbol{g}_0^T \boldsymbol{U}_1^\dagger \boldsymbol{C}\|^2$. Thus, γ_b (cf. Equation (9)) and γ_e (cf. Equation (10)) do not depend on $\boldsymbol{D}$ and $\boldsymbol{E}$.

Next, by substituting (92) for $\boldsymbol{W}$ in (5), we have $P_r \geq P_s(\|\boldsymbol{B}\boldsymbol{U}_2^H \boldsymbol{h}_0\|^2 + \|\boldsymbol{D}\boldsymbol{U}_2^H \boldsymbol{h}_0\|^2) + \sigma_r^2 \text{tr}(\boldsymbol{B}^H \boldsymbol{B} + \boldsymbol{C}^H \boldsymbol{C} + \boldsymbol{D}^H \boldsymbol{D} + \boldsymbol{E}^H \boldsymbol{E})$. Since (P1′) is a secrecy rate maximization problem subject to the given P_r, it turns out that given the optimum secrecy rate, P_r is the minimized required power by taking $\boldsymbol{D} = \boldsymbol{0}$ and $\boldsymbol{E} = \boldsymbol{0}$, while $\boldsymbol{B}$ and $\boldsymbol{C}$ cannot be determined directly. Thus, $\boldsymbol{W} = \boldsymbol{U}_1^\dagger \boldsymbol{B} \boldsymbol{U}_2^H + \boldsymbol{U}_1^\dagger \boldsymbol{C} (\boldsymbol{U}_2^\perp)^H$.

C. Proof of Proposition 3.2

Denoting the dual variable associated with (39a), (39b) and (39c) by λ, α and β_0, respectively, the Lagrangian of (P1′.1-sub2-SDR) is expressed as

$$\begin{aligned}
&L(\chi) = \\
&\text{tr}((P_s \boldsymbol{F}_1 - \lambda \sigma_r^2 \overline{\boldsymbol{Y}}_1 - \alpha P_s \boldsymbol{F}_2 + \alpha \bar{\gamma}_e \sigma_r^2 \overline{\boldsymbol{Y}}_2 - \beta_0 \overline{\boldsymbol{\Phi}}) \boldsymbol{X}) \\
&\qquad + (-\lambda \sigma_b^2 + \alpha \bar{\gamma}_e (q + \sigma_e^2) + \beta_0 P_r) \tau + \lambda,
\end{aligned} \quad (93)$$

where $\chi = \{\boldsymbol{X}, \tau, \lambda, \alpha, \beta_0\}$ denotes the set consisting of all the primal and dual variables. Since problem (P1′.1-sub2-SDR) satisfies the Slater condition, its optimum value admits zero duality gap with its dual counterpart. Furthermore, according to (93), in order for the dual function to be bounded from above, the following constraints must hold:

$$\boldsymbol{Z} = P_s \boldsymbol{F}_1 - \lambda \sigma_r^2 \overline{\boldsymbol{Y}}_1 - \alpha P_s \boldsymbol{F}_2 + \alpha \bar{\gamma}_e \sigma_r^2 \overline{\boldsymbol{Y}}_2 - \beta_0 \overline{\boldsymbol{\Phi}} \preceq \boldsymbol{0}, \quad (94)$$

$$-\lambda \sigma_b^2 + \alpha \bar{\gamma}_e (q + \sigma_e^2) + \beta_0 P_r \leq 0. \quad (95)$$

The dual problem is therefore given by

$$\begin{aligned}
(\text{D-P1}'.\text{1-sub2-SDR}): \min_{\lambda, \alpha, \beta_0} \ & \lambda \\
\text{s.t.} \ & (94), (95), \quad (96a) \\
& (\lambda, \alpha, \beta_0)^T \geq \boldsymbol{0}. \quad (96b)
\end{aligned}$$

It is observed that $\boldsymbol{Z}$ is of the same form as the Hessian matrix with respect to $\boldsymbol{X}$ without rank relaxation. According to [43, Theorem 2.1], $\boldsymbol{Z} \preceq \boldsymbol{0}$ implies that the SDR problem

(P1′.1-sub2-SDR) is tight in this case, i.e., $\exists \boldsymbol{w}^*$ such that $\boldsymbol{X}^* = \boldsymbol{w}^*\boldsymbol{w}^{*H}$. Moreover, since KKT condition necessitates $\boldsymbol{Z}^*\boldsymbol{X}^* = \boldsymbol{0}$, it follows that $\boldsymbol{w}^*$ is the eigenvector corresponds to the zero-eigenvalue of $\boldsymbol{Z}^*$. Hence, we have $\boldsymbol{w}^* = \mu\nu_{\max}(\boldsymbol{Z}^*)$, where $\mu = \sqrt{\frac{P_r}{\mathrm{tr}(\overline{\boldsymbol{\Phi}})\boldsymbol{\nu}_{\max}(\boldsymbol{Z}^*)\boldsymbol{\nu}_{\max}^H(\boldsymbol{Z}^*)}}$ is due to the power constraint of (23c), which completes the proof.

D. Proof of Proposition 4.1

First, given $\tilde{\boldsymbol{h}}_k$, $k = 2, \ldots, K$, fixed, only consider the uncertainty of $\tilde{\boldsymbol{h}}_1$. Since $\|\Delta\tilde{\boldsymbol{h}}_1\|_2^2 \le \epsilon_1''$, we have $1 - \frac{(\Delta\tilde{\boldsymbol{h}}_1^\dagger)^H\Delta\tilde{\boldsymbol{h}}_1^\dagger}{\epsilon_1''} \ge 0$. By applying Lemma 4.2 to (58) with $\boldsymbol{H}_1{}^{(1)} = P_s\boldsymbol{X}'' - \delta\sigma_r^2\boldsymbol{X}' + w^{(0)}\boldsymbol{I}$, $\boldsymbol{F}_1{}^{(1)} = (P_s\boldsymbol{X}'' - \delta\sigma_r^2\boldsymbol{X}')\hat{\tilde{\boldsymbol{h}}}^\dagger$, $\boldsymbol{G}_1{}^{(1)} = \boldsymbol{0}$, $c_1^{(1)} = \hat{\tilde{\boldsymbol{h}}}^T(P_s\boldsymbol{X}'' - \delta\sigma_r^2\boldsymbol{X}')\hat{\tilde{\boldsymbol{h}}}^\dagger - \delta\hat{\tilde{\boldsymbol{h}}}_1^T\boldsymbol{Q}_1\hat{\tilde{\boldsymbol{h}}}_1^\dagger - \delta\sum_{i=2}^K\tilde{\boldsymbol{h}}_i^T\boldsymbol{Q}_i\tilde{\boldsymbol{h}}_i^\dagger - \delta\sigma_b^2 - w^{(0)}N_t\epsilon_0'$, $\boldsymbol{B}_1{}^{(1)} = -\delta\boldsymbol{Q}_1\hat{\tilde{\boldsymbol{h}}}_1^\dagger$, and $\boldsymbol{A}_1{}^{(1)} = -\delta\boldsymbol{Q}_1$, there exists $w^{(1)} \ge 0$ such that the following LMI holds:

$$\begin{bmatrix} \boldsymbol{H}_1^{(1)} & \boldsymbol{F}_1{}^{(1)} & \boldsymbol{G}_1{}^{(1)} \\ \boldsymbol{F}_1{}^{(1)H} & c_1^{(1)} & \boldsymbol{B}_1{}^{(1)H} \\ \boldsymbol{G}_1{}^{(1)H} & \boldsymbol{B}_1{}^{(1)} & \boldsymbol{A}_1{}^{(1)} \end{bmatrix} - w^{(1)}\begin{bmatrix} \boldsymbol{0} & \boldsymbol{0} & \boldsymbol{0} \\ \boldsymbol{0} & 1 & \boldsymbol{0} \\ \boldsymbol{0} & \boldsymbol{0} & \frac{-\boldsymbol{I}}{\epsilon_1''} \end{bmatrix} \succeq \boldsymbol{0}. \tag{97}$$

Note that for $\boldsymbol{Q}_1 \succeq \boldsymbol{0}$, there always exists $w^{(1)} > 0$ such that $\frac{w^{(1)}\boldsymbol{I}}{\epsilon_1''} + \boldsymbol{A}_1{}^{(1)} \succ \boldsymbol{0}$ and we assume that such constraint is applied. According to the property of Schur-Complements [35, A. 5.5], for (97), we have

$$\begin{cases} \begin{bmatrix} \boldsymbol{H}_1{}^{(1)} & \boldsymbol{F}_1{}^{(1)} \\ \boldsymbol{F}_1{}^{(1)H} & c_1^{(1)} - w^{(1)} \end{bmatrix} \\ -\begin{bmatrix} \boldsymbol{G}_1{}^{(1)} \\ \boldsymbol{B}_1{}^{(1)H} \end{bmatrix}\left(\boldsymbol{A}_1{}^{(1)} + \frac{w^{(1)}\boldsymbol{I}}{\epsilon_1''}\right)^{-1}\begin{bmatrix} \boldsymbol{G}_1{}^{(1)H} & \boldsymbol{B}_1{}^{(1)} \end{bmatrix} \succeq \boldsymbol{0}, \\ \frac{w^{(1)}\boldsymbol{I}}{\epsilon_1''} + \boldsymbol{A}_1{}^{(1)} \succ \boldsymbol{0}, \end{cases} \tag{98}$$

which can be reexpressed as

$$\begin{bmatrix} \boldsymbol{A}_1{}^{(1)} + \frac{w^{(1)}\boldsymbol{I}}{\epsilon_1''} & \boldsymbol{G}_1{}^{(1)H} & \boldsymbol{B}_1{}^{(1)} \\ \boldsymbol{G}_1{}^{(1)} & \boldsymbol{H}_1{}^{(1)} & \boldsymbol{F}_1{}^{(1)} \\ \boldsymbol{B}_1{}^{(1)H} & \boldsymbol{F}_1{}^{(1)H} & c_1^{(1)} - w^{(1)} \end{bmatrix} \succeq \boldsymbol{0}. \tag{99}$$

Next, assume that the robust design for (58) has been considered against the precedent $k-1$ uncertainties, i.e.,

$$\begin{bmatrix} \boldsymbol{H}_1{}^{(k-1)} & \boldsymbol{F}_1{}^{(k-1)} & \boldsymbol{G}_1{}^{(k-1)} \\ \boldsymbol{F}_1{}^{(k-1)H} & c_1^{(k-1)} & \boldsymbol{B}_1{}^{(k-1)H} \\ \boldsymbol{G}_1{}^{(k-1)H} & \boldsymbol{B}_1{}^{(k-1)} & \boldsymbol{A}_1{}^{(k-1)} \end{bmatrix} - w^{(k-1)}\begin{bmatrix} \boldsymbol{0} & \boldsymbol{0} & \boldsymbol{0} \\ \boldsymbol{0} & 1 & \boldsymbol{0} \\ \boldsymbol{0} & \boldsymbol{0} & \frac{-\boldsymbol{I}}{\epsilon_{k-1}''} \end{bmatrix} \succeq \boldsymbol{0}, k \ge 2. \tag{100}$$

Applying a similar procedure as that for (97), (100) can be recast as

$$\begin{bmatrix} \frac{w^{(k-1)}\boldsymbol{I}}{\epsilon_{k-1}''} + \boldsymbol{A}_1{}^{(k-1)} & \boldsymbol{G}_1{}^{(k-1)H} & \boldsymbol{B}_1{}^{(k-1)} \\ \boldsymbol{G}_1{}^{(k-1)} & \boldsymbol{H}_1{}^{(k-1)} & \boldsymbol{F}_1{}^{(k-1)} \\ \boldsymbol{B}_1{}^{(k-1)H} & \boldsymbol{F}_1{}^{(k-1)H} & c_1^{(k-1)} - w^{(k-1)} \end{bmatrix} \succeq \boldsymbol{0}. \tag{101}$$

Then given $\tilde{\boldsymbol{h}}_i$, $i = k+1, \ldots, K$ fixed, accommodate the kth uncertainty, i.e., $\tilde{\boldsymbol{h}}_k \in \tilde{\mathcal{H}}_k$, for (101). By applying Lemma 4.2 to the uncertainty of $\tilde{\boldsymbol{h}}_k$, the implication $\|\Delta\tilde{\boldsymbol{h}}_k\|_2^2 \le \epsilon_k'' \Rightarrow$ (101) holds if and only if there exists $w^{(k)} \ge 0$ such that

$$\begin{bmatrix} \boldsymbol{H}_1{}^{(k)} & \boldsymbol{F}_1{}^{(k)} & \boldsymbol{G}_1{}^{(k)} \\ \boldsymbol{F}_1{}^{(k)H} & c_1^{(k)} & \boldsymbol{B}_1{}^{(k)H} \\ \boldsymbol{G}_1{}^{(k)H} & \boldsymbol{B}_1{}^{(k)} & \boldsymbol{A}_1{}^{(k)} \end{bmatrix} - w^{(k)}\begin{bmatrix} \boldsymbol{0} & \boldsymbol{0} & \boldsymbol{0} \\ \boldsymbol{0} & 1 & \boldsymbol{0} \\ \boldsymbol{0} & \boldsymbol{0} & \frac{-\boldsymbol{I}}{\epsilon_k''} \end{bmatrix} \succeq \boldsymbol{0}, \tag{102}$$

where

$$\boldsymbol{H}_1{}^{(k)} = \begin{bmatrix} \boldsymbol{A}_1{}^{(k-1)} + \frac{w^{(k-1)}\boldsymbol{I}}{\epsilon_{k-1}''} & \boldsymbol{G}_1{}^{(k-1)H} \\ \boldsymbol{G}_1{}^{(k-1)} & \boldsymbol{H}_1{}^{(k-1)} \end{bmatrix},$$
$$\boldsymbol{F}_1{}^{(k)} = \begin{bmatrix} \boldsymbol{B}_1{}^{(k-1)} \\ \boldsymbol{F}_1{}^{(k-1)} \end{bmatrix}, \boldsymbol{G}_1{}^{(k)} = \boldsymbol{0}, \tag{103}$$

$c_1^{(k)} = \hat{\tilde{\boldsymbol{h}}}^T(P_s\boldsymbol{X}'' - \delta\sigma_r^2\boldsymbol{X}')\hat{\tilde{\boldsymbol{h}}}^\dagger - \delta\sum_{j=1}^k\hat{\tilde{\boldsymbol{h}}}_j^T\boldsymbol{Q}_j\hat{\tilde{\boldsymbol{h}}}_j^\dagger - \delta\sum_{i=k+1}^K\tilde{\boldsymbol{h}}_i^T\boldsymbol{Q}_i\tilde{\boldsymbol{h}}_i^\dagger - \delta\sigma_b^2 - w^{(0)}N_t\epsilon_0' - \sum_{l=1}^{k-1}w^{(l)}$, $\boldsymbol{B}_1{}^{(k)} = -\delta\boldsymbol{Q}_k\hat{\tilde{\boldsymbol{h}}}_k^\dagger$ and $\boldsymbol{A}_1{}^{(k)} = -\delta\boldsymbol{Q}_k$, $k \ge 2$. Thus, using the method of mathematical induction, (58) holds for $\tilde{\boldsymbol{h}}_k \in \tilde{\mathcal{H}}_k$, $k = 1, \ldots, K$, if and only if there exists $\{w(k) \ge 0\}$, such that (59) is satisfied, which completes the proof.

E. Proof of Proposition 4.2

Taking the similar procedure as that for dealing with (57), the implication $\|\Delta\boldsymbol{g}\|^2 \le N_t\epsilon_0 \Rightarrow$ (62) holds if and only if there exists $v^{(0)} \ge 0$ such that the following LMI holds:

$$\begin{bmatrix} \boldsymbol{H}_2 & \boldsymbol{F}_2 \\ \boldsymbol{F}_2^H & c_2 \end{bmatrix} \succeq \boldsymbol{0}, \tag{104}$$

where $\boldsymbol{H}_2 = -P_s\boldsymbol{X}'' + \bar{\gamma}_e\sigma_r^2\boldsymbol{X}' + v^{(0)}\boldsymbol{I}$, $\boldsymbol{F}_2 = (-P_s\boldsymbol{X}'' + \bar{\gamma}_e\sigma_r^2\boldsymbol{X}')\hat{\boldsymbol{g}}^\dagger$ and $c_2 = \hat{\boldsymbol{g}}^T(-P_s\boldsymbol{X}'' + \bar{\gamma}_e\sigma_r^2\boldsymbol{X}')\hat{\boldsymbol{g}}^\dagger + \bar{\gamma}_e\sum_{k=1}^K\boldsymbol{g}_k^T\boldsymbol{Q}_k\boldsymbol{g}_k^\dagger + \bar{\gamma}_e^2 - v^{(0)}N_t\epsilon_0$. Equation (44a) has been equivalently reformulated into (104). Then, given $\boldsymbol{g}_k$, $k = 2, \ldots, K$, fixed, applying similar procedure to that in Appendix D, it follows that there exists $v^{(1)} \ge 0$ such that the following LMI holds:

$$\begin{bmatrix} \boldsymbol{H}_2^{(1)} & \boldsymbol{F}_2{}^{(1)} & \boldsymbol{G}_2{}^{(1)} \\ \boldsymbol{F}_2{}^{(1)H} & c_2^{(1)} & \boldsymbol{B}_2{}^{(1)H} \\ \boldsymbol{G}_2{}^{(1)H} & \boldsymbol{B}_2{}^{(1)} & \boldsymbol{A}_2{}^{(1)} \end{bmatrix} - v^{(1)}\begin{bmatrix} \boldsymbol{0} & \boldsymbol{0} & \boldsymbol{0} \\ \boldsymbol{0} & 1 & \boldsymbol{0} \\ \boldsymbol{0} & \boldsymbol{0} & \frac{-\boldsymbol{I}}{\epsilon_1} \end{bmatrix} \succeq \boldsymbol{0}. \tag{105}$$

Since $\frac{v^{(1)}\boldsymbol{I}}{\epsilon_1} + \boldsymbol{A}_2{}^{(1)} \succ \boldsymbol{0}$ always holds, (105) is equivalent to the following LMI:

$$\begin{bmatrix} \boldsymbol{A}_2{}^{(1)} + \frac{v^{(1)}\boldsymbol{I}}{\epsilon_1} & \boldsymbol{G}_2{}^{(1)H} & \boldsymbol{B}_2{}^{(1)} \\ \boldsymbol{G}_2{}^{(1)} & \boldsymbol{H}_2{}^{(1)} & \boldsymbol{F}_2{}^{(1)} \\ \boldsymbol{B}_2{}^{(1)H} & \boldsymbol{F}_2{}^{(1)H} & c_2^{(1)} - v^{(1)} \end{bmatrix} \succeq \boldsymbol{0}. \tag{106}$$

Next, devising the method of mathematical induction again as that for (99), (104) holds for $\boldsymbol{g}_k \in \mathcal{G}_k$, $\forall k$, if and only if there exists $\{v(k) \ge 0\}$, such that (63) is satisfied, which completes the proof.

F. Proof of Proposition 4.3

We only sketch the proof herein since it is quite similar to that of Proposition 4.1. First, apply Lemma 4.2 to (71) given $\tilde{\boldsymbol{h}}_k$'s, $k = 2, \ldots, K$, fixed and obtain an initial LMI. Next, manipulate

the resulting LMI according to the property of Schur-Complements to facilitate using Lemma 4.2. Then, repeat this procedure until all the semi-indefinite constraints w.r.t. $\tilde{\boldsymbol{h}}_k$'s have been incorporated into an equivalent LMI.

G. Proof of Proposition 4.5

According to the KKT conditions of (P2′.1-RW-SDR), we have $\bar{\boldsymbol{A}}^*\boldsymbol{X}^* = \boldsymbol{0}$, where $\bar{\boldsymbol{A}}^*$ is given by (79). Define $\bar{\boldsymbol{C}}^* = \bar{\boldsymbol{A}}^* - w_{2,2}^* P_s \hat{\boldsymbol{F}}_1$ with $\mathrm{rank}(\bar{\boldsymbol{C}}^*)$ denoted by $\bar{r}_c$. Then take the similar procedure as Case I and Case II in Appendix A, it can be obtained that $\boldsymbol{X}^* = \sum_{n=1}^{N_t^2-\bar{r}_c} \bar{a}_n \bar{\boldsymbol{\eta}}_n \bar{\boldsymbol{\eta}}_n^H + \bar{b}\bar{\boldsymbol{\xi}}\bar{\boldsymbol{\xi}}^H$.

Next, we prove the second half of Proposition 4.5. According to (81),

$$P_s \mathrm{tr}(\hat{\boldsymbol{F}}_1 \hat{\boldsymbol{X}}^*) = P_s \mathrm{tr}(\hat{\boldsymbol{F}}_1 \boldsymbol{X}^*) \geq \min_{\tilde{\boldsymbol{h}}_0 \in \tilde{\mathcal{H}}_0} P_s \mathrm{tr}(\boldsymbol{F}_1 \boldsymbol{X}) \geq \delta^*, \tag{107}$$

and thus (69a) holds true, which implies that the same optimal value as (P2′.1-RW-SDR), i.e., δ^*, is achievable. However, since the constraint in (68c) is ignored, the global optimal $\bar{\gamma}_e^*$ for (P2′.2) via solving (P2′.1-RW-SDR) is probably violated in (P2′.1-RW-SDR-sub). For example, $\frac{P_s \mathrm{tr}(\boldsymbol{F}_2 \hat{\boldsymbol{X}}^*)}{\sigma_r^2 \mathrm{tr}(\overline{\boldsymbol{Y}}_2 \hat{\boldsymbol{X}}^*) + \sum_{k=1}^K \boldsymbol{g}_k^T \hat{\boldsymbol{Q}}_k^* \boldsymbol{g}_k^\dagger + \hat{\tau}^* \sigma_e^2} = \bar{\gamma}_e^0 \geq \hat{F}(\bar{\gamma}_e^*)$, which results in the actual objective value for (P2′.2), $\frac{1+\hat{H}(\bar{\gamma}_e^*)}{1+\bar{\gamma}_e^0}$ smaller than $\frac{1+\hat{H}(\bar{\gamma}_e^*)}{1+\hat{F}(\bar{\gamma}_e^*)}$, and thus suboptimal for (P2′).

References

[1] L. R. Varshney, "Transporting information and energy simultaneously," in *Proc. IEEE Int. Symp. Inf. Theory (ISIT)*, Toronto, ON, CA, Jul. 2008, pp. 1612–1616.

[2] P. Grover and A. Sahai, "Shannon meets Tesla: Wireless information and power transfer," in *Proc. IEEE Int. Symp. Inf. (ISIT)*, Austin, TX, USA, Jun. 2010, pp. 2363–2367.

[3] R. Zhang and C. K. Ho, "MIMO broadcasting for simultaneous wireless information and power transfer," *IEEE Trans. Wireless Commun.*, vol. 12, no. 5, pp. 1989–2001, May 2013.

[4] X. Zhou, R. Zhang, and C. K. Ho, "Wireless information and power transfer: Architecture design and rate-energy tradeoff," *IEEE Trans. Commun.*, vol. 61, no. 11, pp. 4754–4767, Nov. 2013.

[5] L. Liu, R. Zhang, and K. Chua, "Wireless information transfer with opportunistic energy harvesting," *IEEE Trans. Wireless Commun.*, vol. 12, no. 1, pp. 288–300, Jan. 2013.

[6] J. Xu, L. Liu, and R. Zhang, "Multiuser MISO beamforming for simultaneous wireless information and power transfer," *IEEE Trans. Signal Process.*, vol. 62, no. 18, pp. 4798–4810, Sep. 2014.

[7] L. Liu, R. Zhang, and K.-C. Chua, "Secrecy wireless information and power transfer with MISO beamforming," *IEEE Trans. Signal Process.*, vol. 62, no. 7, pp. 1850–1863, Apr. 2014.

[8] D. W. K. Ng, E. S. Lo, and R. Schober, "Robust beamforming for secure communication in systems with wireless information and power transfer," *IEEE Trans. Wireless Commun.*, vol. 13, no. 8, pp. 4599–4615, Aug. 2014.

[9] H. Xing, L. Liu, and R. Zhang, "Secrecy wireless information and power transfer in fading wiretap channel," *IEEE Trans. Veh. Technol.*, 2015, arXiv:1408.1987.

[10] H. Ju and R. Zhang, "Throughput maximization in wireless powered communication networks," *IEEE Trans. Wireless Commun.*, vol. 13, no. 1, pp. 418–428, Jan. 2014.

[11] H. Xing, Z. Chu, Z. Ding, and A. Nallanathan, "Harvest-and-jam:Improving security for wireless energy harvesting cooperative networks," in *Proc. IEEE Global Commun. Conf. (GLOBECOM)*, Austin, TX, USA, Dec. 2014, pp. 3145–3150.

[12] E. Tekin and A. Yener, "The general Gaussian multiple-access and two-way wiretap channels: Achievable rates and cooperative jamming," *IEEE Trans. Inf. Theory*, vol. 54, no. 6, pp. 2735–2751, Jun. 2008.

[13] L. Dong, Z. Han, A. P. Petropulu, and H. V. Poor, "Improving wireless physical layer security via cooperating relays," *IEEE Trans. Signal Process.*, vol. 58, no. 3, pp. 1875–1888, Mar. 2010.

[14] X. Tang, R. Liu, P. Spasojevic, and H. V. Poor, "The Gaussian wiretap channel with a helping interferer," in *Proc. IEEE Int. Symp. Inf. (ISIT)*, Toronto, ON, CA, Jul. 2008, pp. 389–393.

[15] J. Huang and A. L. Swindlehurst, "Cooperative jamming for secure communications in MIMO relay networks," *IEEE Trans. Signal Process.*, vol. 59, no. 10, pp. 4871–4884, Oct. 2011.

[16] S. Goel and R. Negi, "Guaranteeing secrecy using artificial noise," *IEEE Trans. Wireless Commun.*, vol. 7, no. 6, pp. 2180–2189, Jun. 2008.

[17] G. Zheng, L.-C. Choo, and K.-K. Wong, "Optimal cooperative jamming to enhance physical layer security using relays," *IEEE Trans. Signal Process.*, vol. 59, no. 3, pp. 1317–1322, 2011.

[18] Z. Chu, K. Cumanan, Z. Ding, M. Johnston, and S. Le Goff, "Secrecy rate optimizations for a MIMO secrecy channel with a cooperative jammer," *IEEE Trans. Veh. Technol.*, vol. 64, no. 5, pp. 1833–1847, May 2015.

[19] K. Cumanan, Z. Ding, B. Sharif, G. Y. Tian, and K. K. Leung, "Secrecy rate optimizations for a MIMO secrecy channel with a multiple-antenna eavesdropper," *IEEE Trans. Veh. Technol.*, vol. 63, no. 4, pp. 1678–1690, May 2014.

[20] J. Zhang and M. C. Gursoy, "Relay beamforming strategies for physical-layer security," in *Proc. IEEE Annu. Conf. Inf. Sci. Syst. (CISS)*, Princeton, NJ, USA, Mar. 2010, pp. 1–6.

[21] Y. Yang, Q. Li, W.-K. Ma, J. Ge, and P. Ching, "Cooperative secure beamforming for AF relay networks with multiple eavesdroppers," *IEEE Signal Process. Lett.*, vol. 20, no. 1, pp. 35–38, Jan. 2013.

[22] J. Li, A. P. Petropulu, and S. Weber, "On cooperative relaying schemes for wireless physical layer security," *IEEE Trans. Signal Process.*, vol. 59, no. 10, pp. 4985–4997, Oct. 2011.

[23] X. Wang, K. Wang, and X.-D. Zhang, "Secure relay beamforming with imperfect channel side information," *IEEE Trans. Veh. Technol.*, vol. 62, no. 5, pp. 2140–2155, Jun. 2013.

[24] B. He, X. Zhou, and T. D. Abhayapala, "Wireless physical layer security with imperfect channel state information: A survey," *ZTE Commun.*, vol. 11, no. 3, pp. 11–19, Sep. 2013.

[25] Q. Li and W.-K. Ma, "Optimal and robust transmit designs for MISO channel secrecy by semidefinite programming," *IEEE Trans. Signal Process.*, vol. 59, no. 8, pp. 3799–3812, Aug. 2011.

[26] J. Huang and A. Swindlehurst, "Robust secure transmission in MISO channels based on worst-case optimization," *IEEE Trans. Signal Process.*, vol. 60, no. 4, pp. 1696–1707, Apr. 2012.

[27] Z. Chu, K. Cumanan, Z. Ding, M. Johnston, and S. Le Goff, "Robust outage secrecy rate optimizations for a MIMO secrecy channel," *IEEE Wireless Commun. Lett.*, vol. 4, no. 1, pp. 86–89, Feb. 2015.

[28] Z. Chu, H. Xing, M. Johnston, and S. Le Goff, "Secrecy rate optimizations for a MISO secrecy channel with multiple multi-antenna eavesdroppers," *IEEE Trans. Wireless Commun.*, 2015.

[29] Q. Li, Y. Yang, W.-K. Ma, M. Lin, J. Ge, and J. Lin, "Robust cooperative beamforming and artificial noise design for physical-layer secrecy in AF multi-antenna multi-relay networks," *IEEE Trans. Signal Process.*, vol. 63, no. 1, pp. 206–220, Jan. 2015.

[30] W. Liu, X. Zhou, S. Durrani, and P. Popovski, "Secure communication with a wireless-powered friendly jammer," *IEEE Trans. Wireless Commun.*, 2015, arXiv:1412.0349.

[31] A. Chorti, S. M. Perlaza, Z. Han, and H. V. Poor, "On the resilience of wireless multiuser networks to passive and active eavesdroppers," *IEEE J. Sel. Areas Commun*, vol. 31, no. 9, pp. 1850–1863, Sep. 2013.

[32] A. J. Laub, *Matrix Analysis for Scientists and Engineers*. Philadelphia, PA, USA: SIAM, 2005.

[33] A. Charnes and W. W. Cooper, "Programming with linear fractional functionals," *Naval Res. Logist. Quart.*, vol. 9, no. 3-4, pp. 181–186, Sept.–Dec. 1962.

[34] H. Xing, K.-K. Wong, Z. Chu, and A. Nallanathan, Robust MIMO Harvest-and-jam Helpers and Relaying for Secret Communications [Online]. Available: arXiv:1502.07066.

[35] S. Boyd and L. Vandenberghe, *Convex Optimization*. Cambridge, U.K.: Cambridge Univ. Press, 2004.

[36] Y. Huang and D. P. Palomar, "Rank-constrained separable semidefinite programming with applications to optimal beamforming," *IEEE Trans. Signal Process.*, vol. 58, no. 2, pp. 664–678, Feb. 2010.

[37] R. Zhang, Y.-C. Liang, C. C. Chai, and S. Cui, "Optimal beamforming for two-way multi-antenna relay channel with analogue network coding," *IEEE J. Sel. Areas Commun.*, vol. 27, no. 5, pp. 699–712, Jun. 2009.

[38] Z.-Q. Luo, J. F. Sturm, and S. Zhang, "Multivariate nonnegative quadratic mappings," *SIAM J. Optim.*, vol. 14, no. 4, pp. 1140–1162, 2004.

[39] H. Wang, S. Ma, T.-S. Ng, and H. V. Poor, "A general analytical approach for opportunistic cooperative systems with spatially random relays," *IEEE Trans. Wireless Commun.*, vol. 10, no. 12, pp. 4122–4129, Dec. 2011.
[40] E. Karipidis, N. D. Sidiropoulos, and Z.-Q. Luo, "Far-field multicast beamforming for uniform linear antenna arrays," *IEEE Trans. Signal Process.*, vol. 55, no. 10, pp. 4916–4927, Oct. 2007.
[41] S. Luo, J. Li, and A. Petropulu, "Uncoordinated cooperative jamming for secret communications," *IEEE Trans. Inf. Forens. Secur.*, vol. 8, no. 7, pp. 1081–1090, Jul. 2013.
[42] Y. Liang, H. Poor, and S. Shamai, "Secure communication over fading channels," *IEEE Trans. Inf. Theory*, vol. 54, no. 6, pp. 2470–2492, Jun. 2008.
[43] W. Ai and S. Zhang, "Strong duality for the CDT subproblem: A necessary and sufficient condition," *SIAM J. Optim.*, vol. 19, no. 4, pp. 1735–1756, Feb. 2009.

Hong Xing (S'12) received the B.Eng. degree in electronic sciences and technologies, and the B.A. degree in English both from Zhejiang University (ZJU), Hangzhou, China, in 2011.

She is currently working toward the Ph.D. degree with the Centre for Telecommunications Research, Department of Informatics, King's College London. From November 2012 to March 2014, she was a visiting Ph.D. student with the Department of Electrical and Computer Engineering, National University of Singapore. Her research interests include physical-layer security, wireless information and power transfer, cooperative communications, and applications of convex optimization in wireless communications.

Kai-Kit Wong (M'01–SM'08) received the B.Eng., M.Phil., and Ph.D. degrees, all in electrical and electronic engineering, from the Hong Kong University of Science and Technology, Hong Kong, in 1996, 1998, and 2001, respectively.

He is Full Professor and Chair in Wireless Communications at the Department of Electronic and Electrical Engineering, University College London, United Kingdom. Prior to this, he was on the faculty of the University of Hong Kong and a Lecturer at the University of Hull, as a Research Assistant Professor. He also previously took up visiting positions with the Smart Antennas Research Group of Stanford University, Stanford, CA, USA, and the Wireless Communications Research Department of Lucent Technologies, Bell Labs, Holmdel, NJ, USA

Professor Wong is a Fellow of IET. He has been a Senior Editor of the IEEE COMMUNICATIONS LETTERS since 2012 and is presently serving on the editorial boards of the IEEE WIRELESS COMMUNICATIONS LETTERS (since 2011), IEEE ComSoc/KICS JOURNAL OF COMMUNICATIONS AND NETWORKS (since 2010), IET *Communications* (since 2009), and *Physical Communications* (Elsevier) (since 2012). He also has served as Editor for the IEEE TRANSACTIONS ON WIRELESS COMMUNICATIONS from 2005 to 2011, Review Editor for the IEEE COMMUNICATIONS LETTERS from 2009 to 2012, and Associate Editor for the IEEE SIGNAL PROCESSING LETTERS from 2009 to 2012.

Zheng Chu received the B.Eng. degree from the School of Electric and Information Engineering, Zhengzhou University of Light Industry (ZZULI), in 2007, and the M.Sc. degree from the School of Electric and Electronic Engineering, North China Electrical Power University (NCEPU), in 2011. He received the M.Sc. degree (with distinction) from the School of Electrical and Electronic Engineering, Newcastle University, U.K., in 2012.

Currently, he is pursuing the Ph.D. degree with the Communications, Sensors, Signal, and Information Processing (ComS^{2}IP) Group, School of Electrical and Electronic Engineering, Newcastle University. His research interests include physical layer security, wireless cooperative networks, wireless power transfer, convex optimization techniques, and game theory.

Arumugam Nallanathan (S'97–M'00–SM'05) received the B.Sc. degree with honors from the University of Peradeniya, Sri-Lanka, in 1991, the C.P.G.S. degree from the University of Cambridge, Cambridge, U.K., in 1994, and the Ph.D. degree from the University of Hong Kong, Hong Kong, in 2000, all in electrical engineering.

He is a Professor of Wireless Communications in the Department of Informatics at King's College London, University of London, U.K.. He served as the Head of Graduate Studies in the School of Natural and Mathematical Sciences at King's College London, during 2011–2012. He was an Assistant Professor with the Department of Electrical and Computer Engineering, National University of Singapore, from August 2000 to December 2007. His research interests include 5G Technologies, millimeter wave communications, cognitive radio, and relay networks. In these areas, he coauthored nearly 250 papers.

Dr. Nallanathan is a corecipient of the Best Paper Award presented at the 2007 IEEE International Conference on Ultra-Wideband (ICUWB-2007). He is a Distinguished Lecturer of IEEE Vehicular Technology Society. He is an Editor for the IEEE TRANSACTIONS ON COMMUNICATIONS and the IEEE TRANSACTIONS ON VEHICULAR TECHNOLOGY. He was an Editor for the IEEE TRANSACTIONS ON WIRELESS COMMUNICATIONS (2006–2011), IEEE WIRELESS COMMUNICATIONS LETTERS, and IEEE SIGNAL PROCESSING LETTERS. He served as the Chair for the Signal Processing and Communication Electronics Technical Committee of IEEE Communications Society, Technical Program Co-Chair (MAC track) for IEEE WCNC 2014, Co-Chair for the IEEE GLOBECOM 2013 (Communications Theory Symposium), Co-Chair for the IEEE ICC 2012 (Signal Processing for Communications Symposium), Co-Chair for the IEEE GLOBECOM 2011 (Signal Processing for Communications Symposium), Technical Program Co-Chair for the IEEE International Conference on UWB 2011 (IEEE ICUWB 2011), Co-Chair for the IEEE ICC 2009 (Wireless Communications Symposium), Co-Chair for the IEEE GLOBECOM 2008 (Signal Processing for Communications Symposium), and General Track Chair for IEEE VTC 2008. He received the IEEE Communications Society SPCE Outstanding Service award 2012 and the IEEE Communications Society RCC Outstanding Service award 2014.